OPEN ACCESS Freely available online

PLoS one

Light-evoked Somatosensory Perception of Transgenic Rats That Express Channelrhodopsin-2 in Dorsal Root Ganglion Cells

Zhi-Gang Ji[1,2], Shin Ito[1,2], Tatsuya Honjoh[1,2], Hiroyuki Ohta[1,3], Toru Ishizuka[1], Yugo Fukazawa[4], Hiromu Yawo[1,2,5]*

1 Department of Developmental Biology and Neuroscience, Tohoku University Graduate School of Life Sciences and JST, CREST, Sendai, Japan, **2** Tohoku University Basic and Translational Research Centre for Global Brain Science, Sendai, Japan, **3** Department of Physiology, National Defense Medical College, Tokorozawa, Japan, **4** Department of Anatomy and Molecular Cell Biology, Nagoya University Graduate School of Medicine, Nagoya, Japan, **5** Center for Neuroscience, Tohoku University Graduate School of Medicine, Sendai, Japan

Abstract

In vertebrate somatosensory systems, each mode of touch-pressure, temperature or pain is sensed by sensory endings of different dorsal root ganglion (DRG) neurons, which conducted to the specific cortical loci as nerve impulses. Therefore, direct electrical stimulation of the peripheral nerve endings causes an erroneous sensation to be conducted by the nerve. We have recently generated several transgenic lines of rat in which channelrhodopsin-2 (ChR2) transgene is driven by the Thy-1.2 promoter. In one of them, W-TChR2V4, some neurons were endowed with photosensitivity by the introduction of the ChR2 gene, coding an algal photoreceptor molecule. The DRG neurons expressing ChR2 were immunohistochemically identified using specific antibodies to the markers of mechanoreceptive or nociceptive neurons. Their peripheral nerve endings in the plantar skin as well as the central endings in the spinal cord were also examined. We identified that ChR2 is expressed in a certain population of large neurons in the DRG of W-TChR2V4. On the basis of their morphology and molecular markers, these neurons were classified as mechanoreceptive but not nociceptive. ChR2 was also distributed in their peripheral sensory nerve endings, some of which were closely associated with CK20-positive cells to form Merkel cell-neurite complexes or with S-100-positive cells to form structures like Meissner's corpuscles. These nerve endings are thus suggested to be involved in the sensing of touch. Each W-TChR2V4 rat showed a sensory-evoked behavior in response to blue LED flashes on the plantar skin. It is thus suggested that each rat acquired an unusual sensory modality of sensing blue light through the skin as touch-pressure. This light-evoked somatosensory perception should facilitate study of how the complex tactile sense emerges in the brain.

Citation: Ji Z-G, Ito S, Honjoh T, Ohta H, Ishizuka T, et al. (2012) Light-evoked Somatosensory Perception of Transgenic Rats That Express Channelrhodopsin-2 in Dorsal Root Ganglion Cells. PLoS ONE 7(3): e32699. doi:10.1371/journal.pone.0032699

Editor: Mark L. Baccei, University of Cincinnatti, United States of America

Received October 18, 2011; **Accepted** January 29, 2012; **Published** March 6, 2012

Funding: Funding was provided by the Program for Promotion of Fundamental Studies in Health Sciences of the National Institute of Biomedical Innovation (NIBIO), Japan; Global COE Program (Basic & Translational Research Centre for Global Brain Science), MEXT (Ministry of Education, Culture, Sports, Science, and Technology), Japan; and Strategic Research Program for Brain Sciences (SRPBS), MEXT, Japan. The funders had no role in study design, data collection and analysis, decision to publish, or preparation of the manuscript.

Competing Interests: The authors have declared that no competing interests exist.

* E-mail: yawo-hiromu@m.tohoku.ac.jp

Introduction

Knowledge of the world is obtained exclusively via perception through our sensory systems which consist of peripheral sensory organs, sensory nerves and the central nervous system (CNS). In principle, a sensation is classified according to its modality, that is, the kind of energy inducing physiological transduction in a specific group of sensory organs. For example, in the somatosensory systems, each mode of touch-pressure, temperature or pain is sensed by sensory endings of different dorsal root ganglion (DRG) neurons. Their signals are conducted to a specific cortical locus as nerve impulses, which are then integrated to generate somatosensory perception. Therefore, non-physiological energy transduction such as direct electrical stimulation of a peripheral nerve causes an erroneous sensation to be conducted by the nerve.

In the case of light, rhodopsins are molecules involved in its perception by the photoreceptor cells in the vertebrate retina [1,2]. Each rhodopsin is a seven-pass transmembrane molecule, homologous to G-protein-coupled receptors, and activates cyclic GMP phosphodiesterase upon activation. With the subsequent reduction of the intracellular level of cGMP, the cyclic-nucleotide-gated cation channels are closed [3,4]. A light signal is thus converted into an electrical one through a cascade of at least four molecules. On the other hand, light is perceived by archaea-type rhodopsins, channelrhodopsin-1 (ChR1) and -2 (ChR2), during the light-directed behavior of a unicellular green alga, *Chlamydomonas reinhardtii* [5–9]. Each channelrhodopsin consists of a seven-pass transmembrane apoprotein and a retinal which covalently binds to it. The photoisomerization of all-*trans*-retinal to the 13-*cis* configuration is coupled to conformational changes in the protein that result in increased cation permeability. A light signal is thus converted into an electrical one by a single molecule [10]. Previously, it was reported that neurons were endowed with sensitivity to blue light by introduction of the ChR2 gene [11–13].

This optogenetic method has become a powerful tool for the investigation of neural networks in various animals. It also has potential as a visual prosthesis in case of photoreceptor degeneration [14–16].

Different modalities, such as pain, temperature and touch, are mixed when an animal senses the world through its skin. However, by the selective expression of ChR2 in a subset of nociceptive DRG neurons, the modality-specific circuitry has been optically investigated [17,18]. We have recently generated several transgenic rat lines in which ChR2 transgene is driven by the Thy-1.2 promoter [16]. In one of these lines, W-TChR2V4, some neurons were endowed with photosensitivity by this introduction of ChR2; specifically, these neurons were the retinal ganglion cells, the principal neurons in the cerebral cortex and hippocampus, as well as other brain regions. (Figure S1). In this study, we identified that ChR2 is expressed in a certain population of large neurons in the DRG of a rat from this line. On the basis of their morphology and molecular markers, these neurons were classified as mechanoreceptive but not nociceptive. ChR2 was also found to be distributed in their peripheral sensory nerve endings. As the blue light evoked sensory nerve responses through the skin, it appeared to induce the sense of touch in the rats. It is thus suggested that the sensory modality of the somatosensory system was modified to induce reactivity to blue light in these transgenic rats.

Results

ChR2 expression in DRG

The distribution of ChR2-*Venus* conjugates (ChR2V) was immunohistochemically identified using the W-TChR2V4 line. As shown in Figure 1A, the ChR2V-expressing (ChR2V+) DRG neurons always co-expressed NF200 (111/111 neurons, 100%, Figure 1E), one of the markers of myelinated neurons. On the other hand, almost negligible numbers of the ChR2V+ DRG neurons were positive for calcitonin gene-related peptide (CGRP) (3/279 neurons, 1.1%, Figure 1E) (Figure 1B) or $P2X_3$ (7/161 neurons, 4.3%, Figure 1E) (Figure 1C). Previous studies have shown that some of the myelinated A fibers are also involved in proprioception [19,20]. Parvalbumin (PV), a member of the family of low-molecular-weight calcium-binding proteins, has been shown to be preferentially expressed within large DRG neurons and is considered to be a highly specific molecular marker for primary proprioceptors [21,22]. As shown in Figure 1D, some of the ChR2V+ DRG neurons co-expressed PV (108/253 neurons, 43%, Figure 1E). Although not all NF200-positive neurons were ChR2V+ (111/236, 47%), most of the PV-positive neurons were ChR2V+ (108/115 neurons, 94%) (Figure 1F).

The size of each DRG neuron was evaluated by its average diameter, as summarized in Figure 2. The ChR2V+ DRG neurons (diameter, 43 ± 0.42 μm, $n=212$) were clearly discriminated in terms of size from the CGRP-positive DRG neurons (diameter, 23 ± 0.34 μm, $n=230$), with a statistically significant difference ($P\ll10^{-10}$, two-tailed *t*-test). Their size distribution was also different from that of the $P2X_3$-positive DRG neurons (diameter, 23 ± 0.24 μm, $n=229$; $P\ll10^{-10}$, two-tailed *t*-test), although three $P2X_3$-positive neurons had diameters between 35 and 45 μm. On the other hand, there was no significant difference in size between the CGRP- and the $P2X_3$-positive groups. The NF200-positive neurons ($n=236$) appeared to consist of at least two groups, one with diameters smaller than 30 μm and the other with diameters larger than 30 μm. The ChR2V+ DRG neurons were segregated from the former group but co-localized with the latter.

ChR2 expression in dorsal spinal cord

In the dorsal spinal cord, the gray matter has been anatomically classified into five discrete layers [23]. As shown in Figure 3A–C, the ChR2V was broadly distributed in the spinal cord gray matter (see also Figure S2). However, it was negligible in the outer dorsal layers where CGRP immunoreactivity was present (Figure 3B). Similarly, the ChR2V was not co-localized with $P2X_3$ immunoreactivity in the inner dorsal layers (Figure 3C). On the other hand, the distribution of ChR2V overlapped with that of NF200 immunoreactivity (Figure 3A).

ChR2 expression in the peripheral nerve endings

As previously noted, ChR2 was expressed in large DRG neurons, which have been suggested to be involved in proprioception and touch-pressure sensing. The above results showed that only a subpopulation of ChR2V+ DRG neurons co-expressed PV, a marker of proprioceptive neurons. Therefore, it is probable that another subpopulation of these neurons have myelinated nerves involved in touch-pressure, which project their peripheral endings to the skin as mechanoreceptors. In the superficial layer of the skin, indeed, the ChR2V+ nerve bundles were also positive for myelin basic protein (MBP), which is a marker of myelinated axons (Figure 4A). Some of the peripheral endings of mechanoreceptive neurons have been shown to be associated with Merkel cells, which specifically express cytokeratin-20 (CK20), and form Merkel corpuscles in the skin [24], or with lamellar cells of Meissner's corpuscles, which express S-100 [25]. As shown in Figures 4B and 4C, ChR2V+ nerve endings were frequently associated with CK20-positive Merkel cells or with S-100-positive cells to form structures morphologically reminiscent of Meissner's corpuscles. On the other hand, they were not co-localized with the CGRP-positive free nerve endings assumed to be involved in nociception (Figure 4D). Peripherally, some of the proprioceptive DRG neurons projected to the intrafusal muscles as sensory spiral endings. As shown in Figure 4E, ChR2V+ nerve endings were frequently found in muscle. Some of them were motor nerve terminals as the spinal motor neurons also expressed ChR2V (Figure S2). Others were found in the muscle spindles with spiral appearances and co-expressed PV (Figure 4E).

Sensitivity to blue light

We next evaluated the sensitivity of ChR2V+ DRG neurons to blue light. For this evaluation, the DRG neurons were cultured and the ChR2V expression was identified by the presence of *Venus* fluorescence. Under whole-cell voltage clamp, blue LED light pulse evoked a photocurrent in every ChR2V+ neuron (24/24 neurons) (Figure 5A). Both the peak and the steady-state photocurrents were dependent on the light power density (Figure 5B). The peak current ranged between -0.5 and -5.2 nA ($n=24$) at the maximal irradiance, although unclamped currents from escaped action potentials were frequently observed. Under the current clamp, the blue LED light pulse (200 ms) evoked rapid membrane depolarization in an intensity-dependent manner and, eventually, only one action potential in 16 of 18 experiments (Figure 5C). In the remaining two cases, the blue LED light evoked subthreshold depolarization even at the maximum irradiance. The size of the action potential varied from cell to cell (range, 15–72 mV, $n=16$) with threshold irradiances of 0.06–1.3 $mWmm^{-2}$ (Figure 5D). However, the same blue LED light did not evoke any current or voltage response in the ChR2V-negative (ChR2V−) DRG neurons ($n=3$, Figure S3).

When short LED pulses (duration, 20 ms) were repeatedly applied at the maximal irradiance (1.6 $mWmm^{-2}$), they robustly evoked action potentials at low frequency (Figures 5E and 5F). For

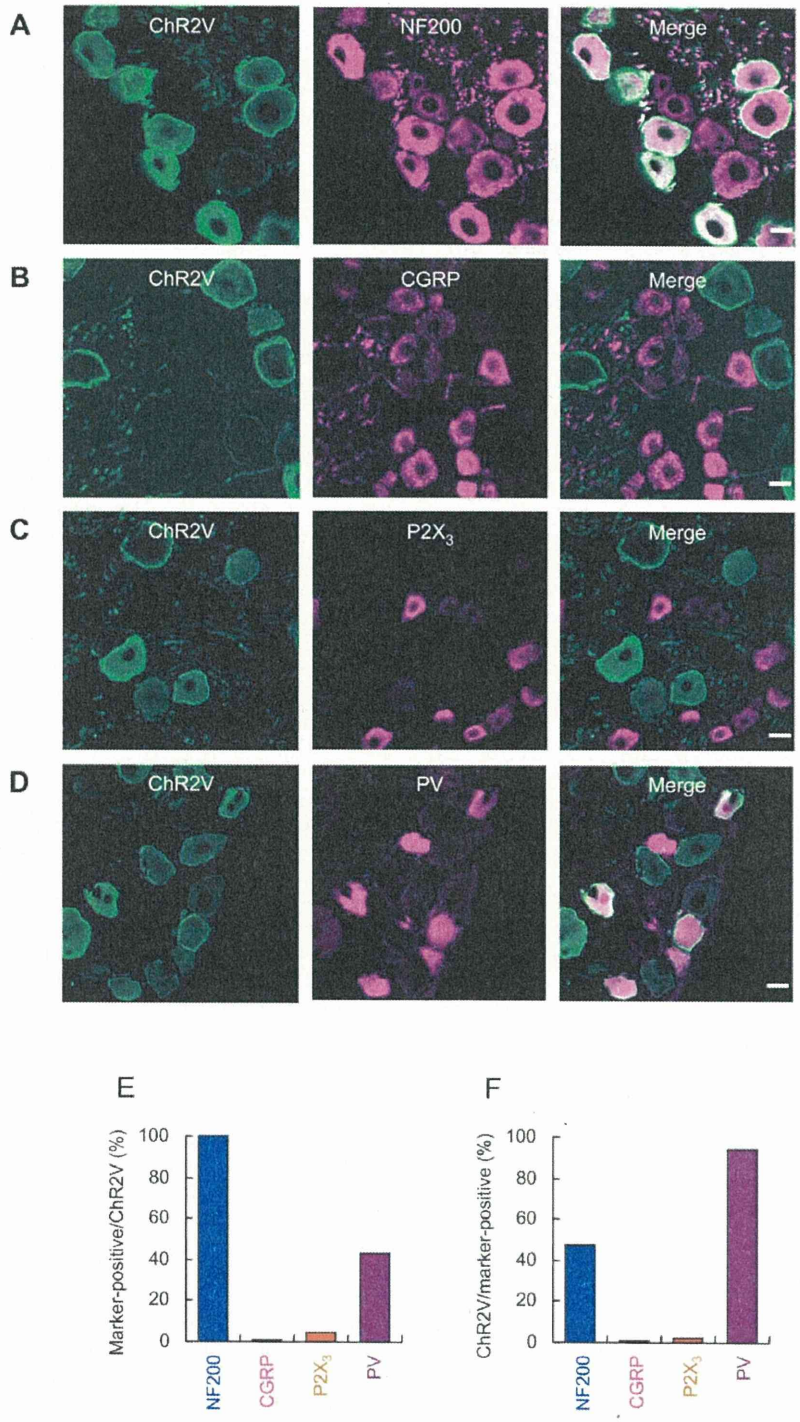

Figure 1. Distribution of channelrhodopsin 2-*Venus* conjugates (ChR2V) in the dorsal root ganglion (DRG) of W-TChR2V4 rats. A–D. Immunohistochemical identification of ChR2V-expressing neurons using cell-type specific markers, NF200 (A), CGRP (B), $P2X_3$ (C) and PV (D). Scale bars indicate 20 μm. E. Probability of the co-expression of each marker, NF200, CGRP, $P2X_3$ or PV, in the ChR2V+ neurons. F. Probability of the co-expression of ChR2V in the neurons positive for each marker, NF200, CGRP, $P2X_3$ or PV.
doi:10.1371/journal.pone.0032699.g001

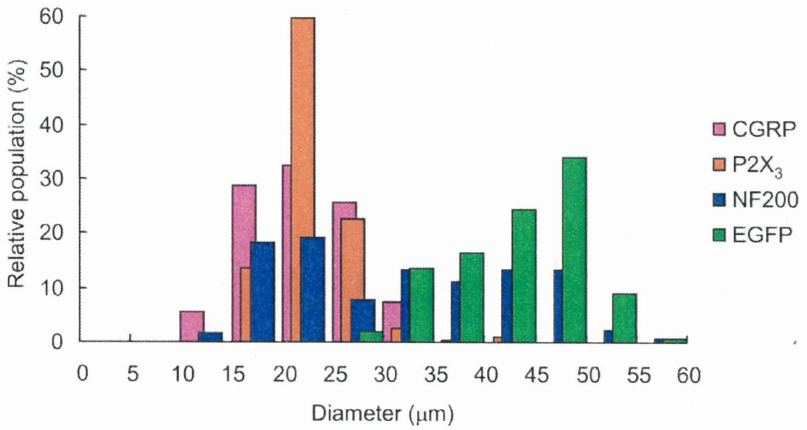

Figure 2. The average diameters of DRG neurons were compared among four groups positive for ChR2V (green), NF200 (blue), CGRP (magenta) and $P2X_3$ (orange).
doi:10.1371/journal.pone.0032699.g002

example, there was no failure of the action potential in 13/14 neurons at 1 Hz, 12/14 at 2 Hz and 10/14 at 5 Hz. However, the fidelity was reduced at increased frequencies: 6/14 at 10 Hz and 3/14 at 20 Hz.

Behavioral responses to light

On the basis of the above evidence, we could expect that the blue light on the plantar skin evokes tactile perception in this transgenic rat. To test this, hindpaws of rats were illuminated at the plantar skin by a series of blue or red LED flashes (duration, 50 ms; 10 pulses at 10 Hz; interval, 10 s) while the rest of the body was shaded with a black cloth (Figure 6A). Although the rats remained quiet, the ChR2V+ rats appeared to move the paw in response to the blue LED flash on its plantar skin (Video S1). The

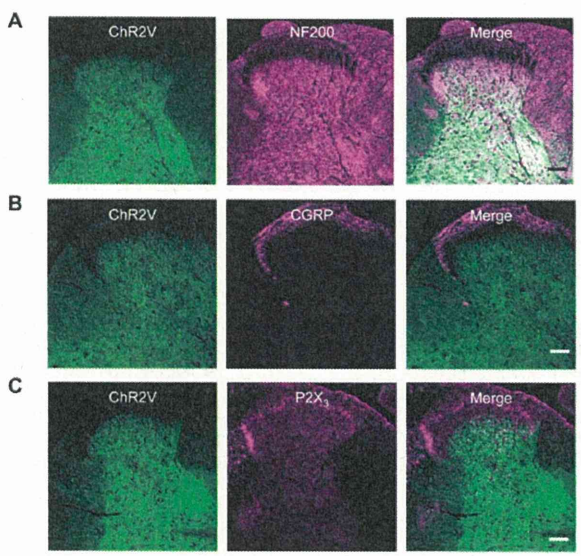

Figure 3. Distribution of ChR2V in the dorsal part of the spinal cord. A–C. Immunohistochemical localization of ChR2V with the cell-type specific markers, NF200 (A), CGRP (B) or $P2X_3$ (C). Scale bars indicate 40 μm.
doi:10.1371/journal.pone.0032699.g003

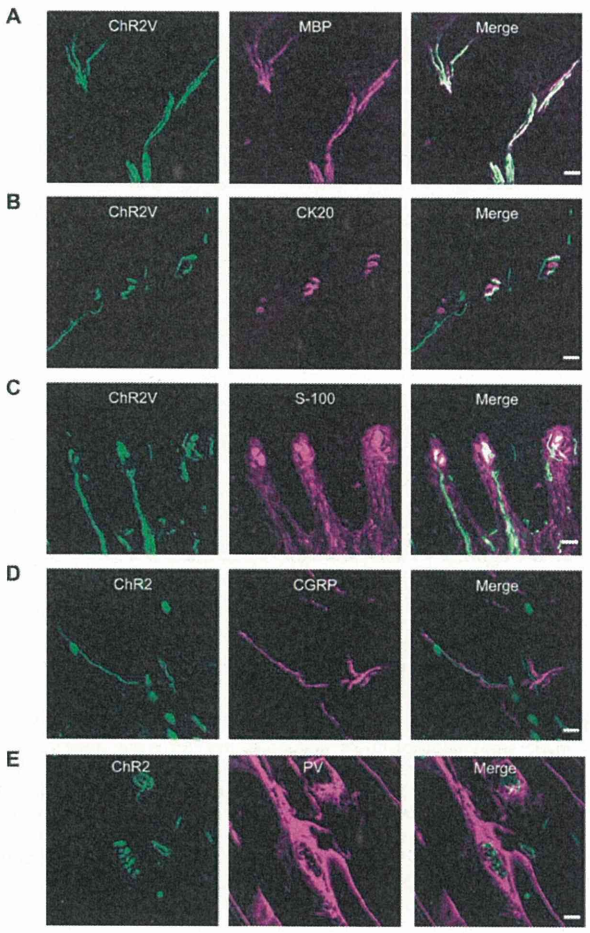

Figure 4. Distribution of ChR2V in the peripheral sensory nerve endings. A–D. Immunohistochemical identification of the ChR2V+ nerve endings in the skin in relation to MBP (A), CK20 (B), S-100 (C) or CGRP (D). E. Co-localization of the ChR2V+ nerve endings with PV in the muscle spindle. Scale bars indicate 20 μm.
doi:10.1371/journal.pone.0032699.g004

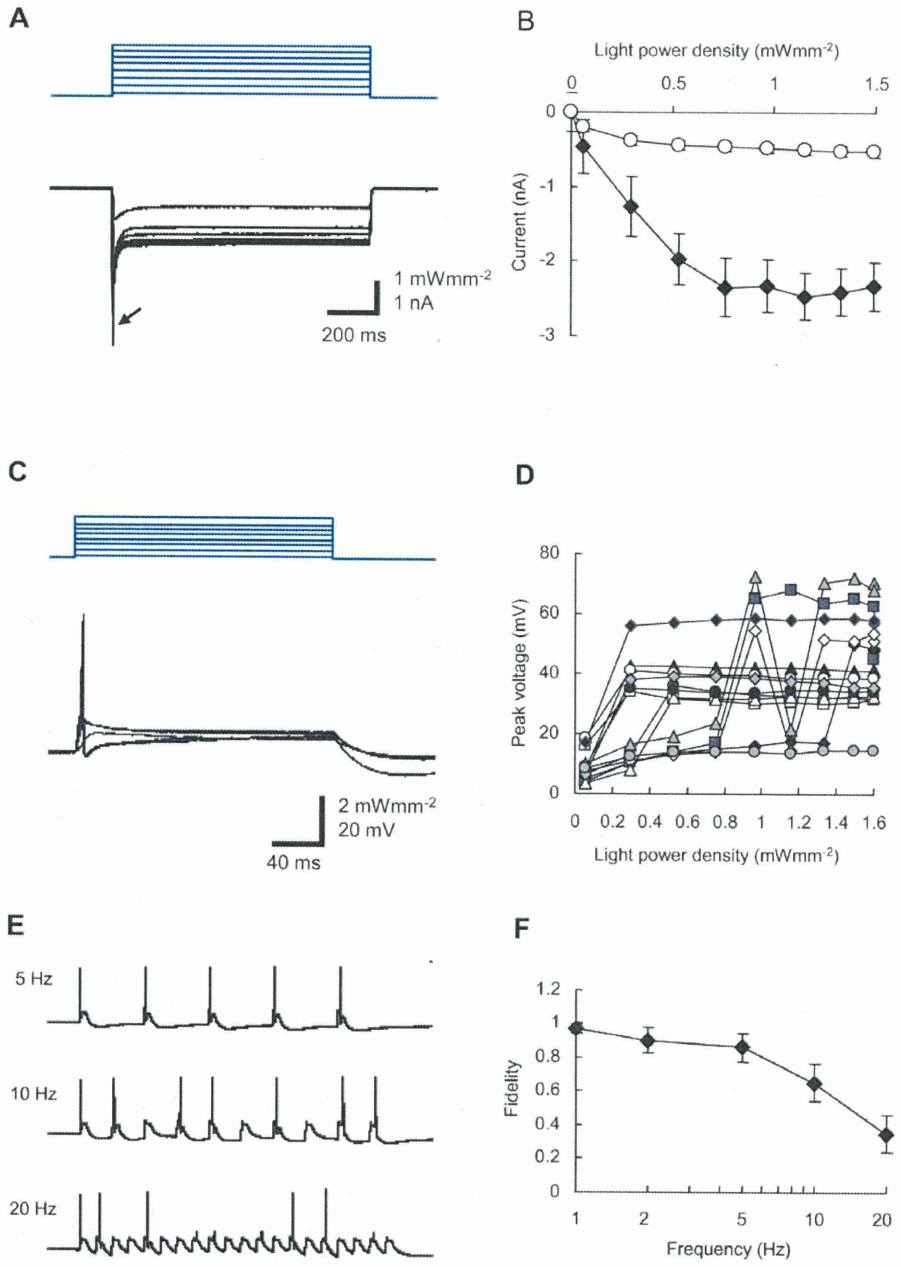

Figure 5. Optical responses of the ChR2V+ DRG neurons. A. Representative records of photocurrents (bottom) evoked by blue LED light of variable strength (top) under voltage clamp. An arrow indicates the unclamped current from escaped action potentials. B. The peak (closed diamonds) and the steady-state (open squares) photocurrent amplitudes (mean ± SEM, both n = 24) as functions of the light power density. C. Representative records of the neuronal membrane potential evoked by blue LED pulses (200 ms) of variable strength under current clamp. The resting membrane potential, −56 mV. D. The maximal voltage changes as a function of the light power density (n = 16). E. Representative records of membrane potential responses of a ChR2V-expressing DRG neuron to the repeated flashing of blue LED pulses (1.6 mWmm^{-2}, 20 ms duration) at various frequencies, that is, 5 Hz (top), 10 Hz (middle) and 20 Hz (bottom). F. Fidelity of generation of action potentials as a function of frequency (mean ± SEM, n = 14).
doi:10.1371/journal.pone.0032699.g005

blue LED flashes clearly and robustly evoked reflexive movements of the paw or toe, whereas the red LED flashes did not (Video S2). The movements during flashing exposure were scored according to their magnitudes (Table 1). The proportion of cases when movement occurred during flashing with blue light was 100%, whereas it was 25±68% with red light, showing a significant difference ($P<0.05$, Wilcoxon signed-rank test, n = 8 animals). Relatively large movements (score, 2–3) were frequently evoked by the blue LED flashes (Figure 6B). There was a significant difference between blue and red flashes (n = 8, $P<0.01$, Wilcoxon

signed-rank test) when we compared the average scores given for the magnitude of movement (Figure 6C). As a control, neither blue nor red flashes evoked clear movements in the case of ChR2V− rats (n = 8). Compared with the ChR2V+ rats, the probability of showing large movements (score 2–3) and the average movement scores of the control rats were negligible (Figures 6B and 6C, $P<0.005$, Mann-Whitney *U*-Test). Similarly, the ChR2V+ rats moved their forepaws significantly more frequently and vigorously during blue LED flash than during red LED flashes (Figures 6D and 6E; Videos S3 and S4). We also tested the light-evoked movement of tails, but only one ChR2V+ rat showed clear responses to the blue LED flashes (Video S5).

Discussion

In this study, we found that ChR2 is expressed in a certain population of large neurons in the DRG of a transgenic rat line, W-TChR2V4, in which the ChR2V transgene was driven by the Thy-1.2 promoter [16]. The ChR2V+ neurons co-expressed NF200, a marker of medium–large neurons involved in mecha-

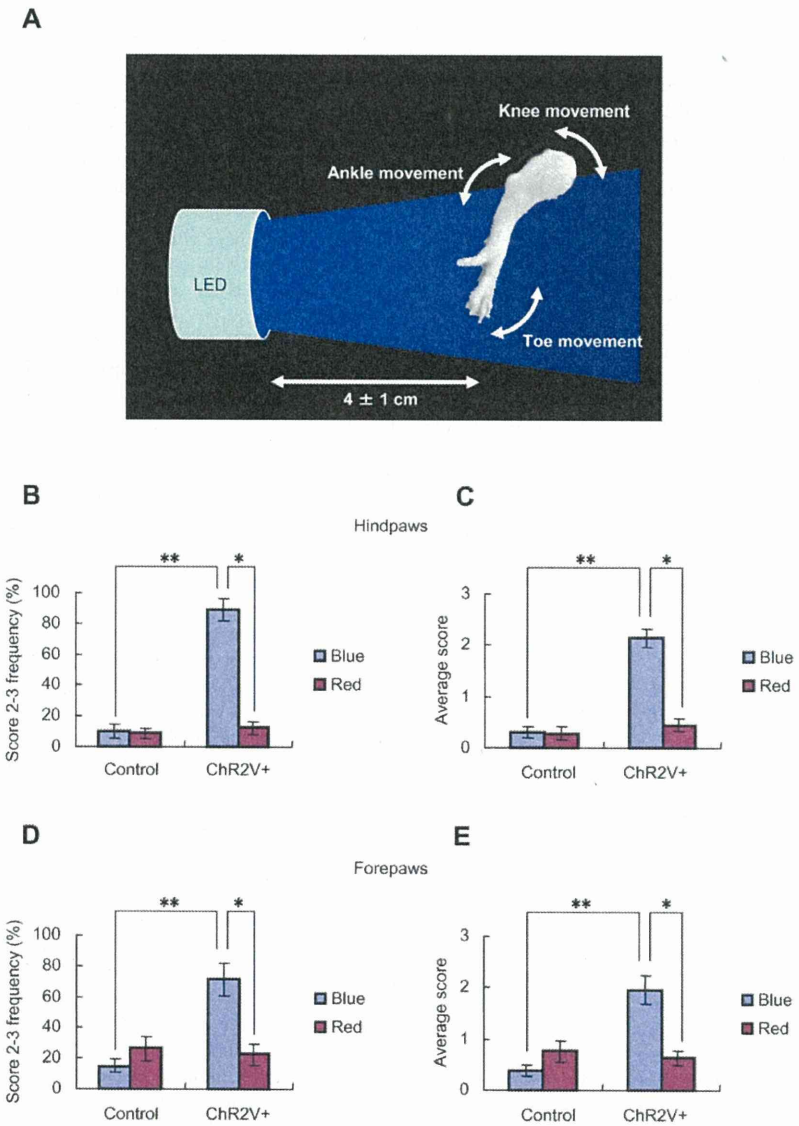

Figure 6. Optically evoked behavioral responses. A. Schematic diagram of the experimental setup. One of four paws was placed in the light path of a blue or red LED so that the plantar skin faced the light while the rest of the body was covered with a black cloth. The distance between the surface of the collimator lens of the LED and the plantar skin was set to about 4 cm, but the exact distance was in the range of 3–5 cm because of the spontaneous movements of the paw. All the experiments were carried out under yellow, dim background light. The optically evoked behavioral responses were scored according to the movement around joints: toe, ankle/wrist or knee/elbow (Table 1). B and C. Light-evoked responses of hindpaws were compared between the wild-type (n = 8) and the ChR2V+ rats (n = 8). The probability of large movements (score 2–3, B) or the average score over ten successive tests (C) was compared between blue and red LED light. D and E. Light-evoked responses of forepaws of the same group of rats: the probability of large movements (score 2–3, D) or the average score (E). Wicoxon signed-rank test was applied for the paired data (*, $P<0.01$) and Mann-Whitney *U*-test for unpaired data (**, $P<0.0005$).
doi:10.1371/journal.pone.0032699.g006

Table 1. The behavioral response score.

Behavior	Score
No response	0
Toe movements	1
Ankle or wrist movements	2
Knee or elbow movements	3

doi:10.1371/journal.pone.0032699.t001

noreception, but not CGRP or $P2X_3$, markers of small neurons involved in nociception. Since the peripheral sensory nerve endings also expressed ChR2, it was expected that photostimulation would evoke action potentials in them. Indeed, the ChR2V+ rats showed sensory-evoked behaviors in response to blue LED flash on their plantar skin. It is thus suggested that the rats had acquired an unusual sensory modality enabling them to sense blue light through the skin.

ChR2V+ DRG neurons are not involved in nociception

The DRG comprises cell bodies of functionally distinct sensory nerves. The DRG neurons have been classified in terms of various characteristics, for example, fast-conducting vs. slow-conducting, myelinated vs. non-myelinated, nociceptive vs. non-nociceptive or small vs. large. In this study, we used NF200 as a marker of myelinated neurons and found that almost all ChR2V+ DRG neurons co-expressed NF200. On the other hand, some NF200-expressing DRG neurons were ChR2V−. It is thus suggested that the ChR2V-expressing DRG neurons are a subpopulation of the fast-conducting myelinated neurons.

The nociceptive neurons can be further classified into peptidergic and non-peptidergic neurons. The peptidergic neurons are immunoreactive to substance P (SP) or CGRP, whereas the non-peptidergic neurons are immunoreactive to isolectin B4 (IB4) or purinergic receptor $P2X_3$ [26–28]. We found that almost all the ChR2V+ neurons were negative for both CGRP and $P2X_3$. Therefore, the nociceptive DRG neurons appeared to be mostly ChR2V−.

In our study over 98% of the ChR2V+ DRG neurons had diameters larger than 30 μm. Although the neuron size is dependent on the age or the body size of the rat, these neurons were classified as medium–large [29–31]. On the other hand, the nociceptive neurons that expressed either CGRP or $P2X_3$ were mostly small. The size distribution of ChR2V+ neurons appeared to be distinct from that of nociceptive neurons. However, a small number of medium-sized DRG neurons were also positive for $P2X_3$. A subpopulation of NF200-expressing DRG neurons were discriminated from ChR2V+ DRG neurons by their small size (diameter$<$30 μm). It is possible that these DRG neurons were small myelinated Aδ-fiber neurons involved in pain [32]. These observations are consistent with the notion that the ChR2V+ neurons are not involved in nociception [33,34], although further studies are necessary to confirm this.

In the spinal cord, neurons involved in nociception are located in the marginal layer (lamina I) and the substantia gelatinosa (lamina II) of the dorsal horn and receive inputs from the nociceptive DRG neurons [35,36]. Indeed, various noxious stimuli induce acute c-Fos expression in these laminae [37]. On the other hand, the myelinated fibers involved in mechanoreception are projecting predominantly to laminae III–V [35–38]. Consistent with these previous studies, immunoreactivity to CGRP or $P2X_3$ was predominantly present in laminae I and II and that to NF200 was negligible in these superficial layers. We found that the ChR2V expression co-localized with neither with CGRP nor $P2X_3$. It is thus suggested that the ChR2V+ fibers are myelinated and involved in mechanoreception.

We also found in the plantar skin that the ChR2V+ nerve fibers were mostly associated with MBP immunoreactivity. It is thus suggested that these fibers were myelinated and distinct from the nociceptive C-fibers that were unmyelinated. They are also unlikely to be nociceptive Aδ fibers that had lost their myelin before entering the skin [39]. On the other hand, ChR2V-positive nerve endings were frequently associated with Merkel cells in the dermis or with S-100-positive cells to form structures like Meissner's corpuscles, suggesting their involvement in the sense of touch-pressure. However, we did not find the axon terminals in the deep mechanoreceptive structures such as Pacinian corpuscles; this was probably because our histological studies were limited to the superficial layer of the plantar skin. Some of the ChR2V+ fibers appeared to be involved in proprioception since they innervated the muscle spindle to form stretch receptors that were PV-positive.

Taken together, the above histological characteristics suggest that ChR2V was not expressed in most nociceptive DRG neurons. Rather, it appeared to be expressed in a subpopulation of mechanoreceptive neurons with myelinated fibers [40]. Some of the ChR2V+ neurons appeared to be involved in proprioception in muscles, tendons and joints since they were also positive for PV. However, others may have innervated the skin and been involved in the sense of touch-pressure.

Light-evoked somatosensory responses

The above findings that the mechanoreceptive DRG neurons expressed ChR2V in both the soma and peripheral endings raised the possibility that the ChR2V+ rats can sense blue light on their skin as if it were a touch. There is further evidence to support this. First, the ChR2V+ DRG neurons were photosensitive and optically depolarized to evoke action potentials. The action potential was generated at the onset of the light pulse and not thereafter, a trait frequently found in mechanoreceptive DRG neurons [41–45]. Second, the ChR2V+ rats moved their paws in response to the blue LED flashes on the plantar skin, but not in response to the red LED flashes. This behavior was not observable in the control ChR2V− rats. Therefore, the light-evoked behaviors were dependent on both the expression of ChR2 and the wavelength (470±17 nm) that is optimal for the activation of ChR2 [9]. As ChR2V was exclusively expressed in the myelinated nerve endings that were non-nociceptive, the blue light was likely to have induced the sense of touch-pressure in the rats. This blue light-evoked response was not clear in other parts of the body such as the tail. It is possible that fur covering the skin would obstruct the penetration of light. Although ChR2V was expressed in motor neurons and their terminals in our rat model (Figure S2), the sensory nerve endings, which lie in the superficial layer of the skin, are expected to be differentially photostimulated because the blue light cannot penetrate deep into the muscle. It is thus suggested that the sensory modality of the somatosensory system was modified so as to be also reactive to blue light in the ChR2V+ rats.

Conclusions

In this work, we have generated an optogenetic rat model that can be used for the research of the somatosensory system. Using ChR2V+ rats, we can discretely photostimulate the mechanoreceptive nerve endings without any effects on the nociceptive free nerve endings. Combined with electrophysiological as well as neuroimaging methods such as fMRI, our rat model should

facilitate study of how complex tactile perception, such as for texture, size and shape, is generated.

Materials and Methods

Ethics Statement

All animal experiments were approved by the Tohoku University Committee for Animal Experiments (Approval No. 2011LsA-23) and were carried out in accordance with the Guidelines for Animal Experiments and Related Activities of Tohoku University as well as the guiding principles of the Physiological Society of Japan and the National institutes of health (NIH), USA.

Animals

The experiments were carried out using offspring of one of the Thy-1 promotor-ChR2-*Venus* transgenic rat lines, W-TChRV4 with the background of Wistar rats [16] mated with wild-type Wistar rat. The littermates were screened by genomic PCR using the appropriate primers (Figure S4), and were determined to be either transgene-positive (ChR2V+) or -negative (ChR2V−). Alternatively, the tip of the tail was freshly examined under fluorescent microscopy to determine whether *Venus* fluorescence was present in the nerve bundle in the tissue (Figure S5). The number of animals in this study was kept to a minimum and, when necessary, all animals were anesthetized to minimize their suffering. Animals had access to food and water ad libitum and were kept under a 12-hour light-dark cycle.

Immunohistochemistry

ChR2V+ rats (five weeks old) were used for the immunohistochemical experiments. They were anesthetized with a ketamine (50 mg/ml, Daiichi Sankyo Co. Ltd., Tokyo, Japan)-xylazine (xylazine hydrochloride, 10 mg/ml, Sigma-Aldrich, St. Louis, MO, USA) mixture (1 ml/kgBW) and transcardially perfused with phosphate-buffered saline (PBS; pH 7.4), followed by 100 ml of 4% paraformaldehyde (PFA) and 0.2% picric acid in PBS. The lumber region of spinal cords together with DRGs, the intercostals muscles and the pedal skin from one of the paws were removed and post-fixed in 4% PFA overnight at 4°C. After cryoprotection through a graded series of sucrose replacements (10%, 20% and 30% in PBS) at 4°C, each tissue was embedded in OCT Compound (4583, Sakura Finetek, Tokyo, Japan) and stored at −80°C.

The localization and cell type of ChR2V-expressing neurons in the tissue were immunohistochemically investigated using anti-EGFP antibody along with the antibody of one of the cell-type-specific markers. Briefly, each frozen section was cut at 16 μm thickness with a cryostat (CM 3050 S, Leica, Wetzlar, Germany), mounted on poly-L-lysine coated slides (Matsunami Glass Ind. Ltd., Kishiwada, Japan) and left to air-dry for 90 min at room temperature. After washing with PBS, slices were incubated for 1 hr in blocking PBS containing 2.5% goat serum, 0.25% carrageenan and 0.1% Triton X-100 at room temperature. Then, the specimens were reacted overnight at 4°C with the primary antibody: rabbit anti-EGFP (1:2,000) [46]; mouse monoclonal anti-NF200 (1:500, N0142, Sigma-Aldrich); rabbit anti-CGRP (1:2,000, C8198, Sigma-Aldrich); guinea-pig anti-CGRP (1:1000, Progen Biotechnik GmbH, Heidelberg, Germany); guinea-pig anti-$P2X_3$ (1:1,000, GP10108, Neuromics, Edina, MN, USA); mouse anti-PV (1:2,000, P3088, Sigma-Aldrich); chicken anti-MBP (1:500, PA1-10008, Thermo Fisher Scientific K.K., Yokohama, Japan), mouse anti-CK20 (1:20, IT-Ks 20.8, Progen Biotechnik GmbH) and mouse anti-S100 (β-subunit) (1:1000, S2532, Sigma-Aldrich). In some specimens, the *Venus* fluorescence signal could be directly examined without any amplification as previously described [47,48]. After 10-min washing three times, the slices were reacted for 1 hr (room temperature) or overnight (4°C) with the combination of the following secondary antibodies (Molecular Probes products from Life Technologies Co., Carlsbad, CA, USA, except for Dylight-549): Alexa Fluor 488-conjugated donkey anti-rabbit IgG (1:500), Alexa Fluor 546-conjugated donkey anti-mouse IgG (1:500), Alexa Fluor 546-conjugated donkey anti-rabbit IgG (1:500) and Alexa Fluor 633-conjugated goat anti-guinea pig IgG (1:500), and Dylight 549-conjugated goat anti-chicken IgY (Thermo Fisher Scientific K.K., 1:100). After washing three times in PBS, the specimens were mounted with Permafluor (Thermo Fisher Scientific K.K.). Images were digitally captured under conventional confocal laser-scanning microscopy (LSM510META, Carl Zeiss, Oberkochen, Germany) and were corrected for brightness and contrast using LSM Image Browser version 3.2 (Carl Zeiss), Photoshop version 6.0 (Adobe Systems Inc, San Jose, CA, USA) and ImageJ (http://rsbweb.nih.gov/ij/). The diameter of a DRG neuron was microscopically measured as the mean of the shortest and longest diameters.

Culture

The DRG neurons of ChR2V+ rats (3–4 weeks) were cultured according to a method reported previously [49] with some modifications. After decapitation, the DRGs from all available spinal levels were taken out and put into an ice-cold dissecting solution. Each DRG was cleaned of the surrounding connective tissue, cut into small pieces and immersed in an enzymatic solution containing 1.0 mg/ml collagenase II (C6885, Sigma-Aldrich), 0.5 mg/ml trypsin (15090-046, a Gibco product from Life Technologies Co.) and 0.1 mg/ml DNase I (Sigma-Aldrich) for 30–45 min at 37°C. The neurons were washed twice with trituration solution containing 2 mg/ml BSA (A7906, Sigma-Aldrich), resuspended in culture medium containing DMEM (D5030, Sigma-Aldrich) supplemented with 3.7 mg/ml $NaHCO_3$, 1 mg/ml D-glucose, 2 mM L-glutamine (G7513, Sigma-Aldrich), 1% penicillin/streptomycin (P0781, Sigma-Aldrich) and 10% FBS (04-001-1, Biological Industries, Beit-Haemek, Israel), and then plated and cultured at 37°C in a humidified incubator with a 95% air and 5% CO_2 atmosphere. The culture medium was changed every two days. The whole-cell recording experiments were carried out within 4–5 days of plating.

Electrophysiology

ChR2V+ DRG neurons were identified under conventional epi-fluorescence microscopy (BH2-RFC, Olympus Optical Co., Tokyo, Japan) equipped with a 40× water-immersion objective (LUMplanP1/IR40×, Olympus) and a conventional filter cube (excitation, 495 nm; dichroic mirror, 505 nm; barrier filter, 515 nm). Electrophysiological recording was performed at 34±2°C (UTC-1000, Ampere Inc., Tokyo, Japan) under whole-cell patch clamp from the soma using an amplifier (EPC 8, HEKA Elektronik Dr. Schulze GmbH, Germany) and computer software (pCLAMP 9, Molecular Devices, LLC, Sunnyvale, CA). The bath solution was composed of (in mM) 138 NaCl, 3 KCl, 2 $CaCl_2$, 1 $MgCl_2$, 4 NaOH, 10 HEPES, 11 glucose, and was adjusted at pH 7.4 by 1 N HCl. The patch pipette solution was composed of (in mM) 125 K-gluconate, 10 KCl, 0.2 EGTA, 10HEPES, 1 $MgCl_2$, 3 MgATP, 0.3Na_2GTP, 10 Na_2-phosphocreatine and 0.1 leupeptin, and was adjusted at pH 7.2 by 1 N KOH. For the optical actuation of a DRG neuron we used a blue LED (470±25 nm wavelength, LXHL-NB98, Philips Lumileds Lighting Co., San Jose, CA, USA) regulated by a pulse generator (SEN-7203, Nihon Kohden, Tokyo, Japan) and computer software

(pCLAMP 9, Molecular Devices, LLC). The maximal light power density of the LED light was 1.6 $mWmm^{-2}$ at the focus.

Behavioral test

Light-dependent behavior was investigated using eight ChR2V-expressing (ChR2V+) (9–21 weeks) and eight non-expressing (ChR2V−) rats, including three littermates (8–14 weeks) and five wild-type Wistar rats (15 weeks). The whole body of a rat, except for one of the four paws and the tail, was shaded from the light with a black cloth. Either a blue (470±17 nm, LXML-PB01-0023, Philips Lumileds Lighting Co.) or a red LED (627±15 nm, LXML-PD01-0030, Philips Lumileds Lighting Co.) was driven by a pulse generator (SEN-7203, Nihon Kohden, Tokyo, Japan) and a DC voltage/current generator/calibrator (R6243, Advantest, Tokyo, Japan). A series of flashes (duration, 50 ms; 10 pulses at 10 Hz; interval, 10 s) was subjected to the skin at a distance of 3–5 cm while the behavior of the rat was captured using a video camera (PC1249, Canon, Tokyo, Japan). All experiments were carried out under yellow, dim background light. The light power density was directly measured using a thermopile (MIR-100Q, Mitsubishi Oil Chemicals, Tokyo, Japan), and was 3–8 $mWmm^{-2}$ at the skin for both the blue and the red LED lights. Under double-blind conditions, the response to light was scored as described in Table 1.

Supporting Information

Video S1 Typical ChR2V+ transgenic rat showed sensory-evoked behavior of a hindpaw in response to a series of blue LED flashes on the plantar skin as if it had been touched.
(MPG)

Video S2 The same hindpaw showed no specific response to a train of red LED flashes.
(MPG)

Video S3 The same rat also showed sensory-evoked behavior of a forepaw in response to a train of blue LED flashes.
(MPG)

Video S4 The same forepaw showed no specific response to a train of red LED flashes.
(MPG)

Video S5 The same rat also showed clear sensory-evoked movement of its tail in response to a train of blue LED flashes as if it had been touched.
(MPG)

Figure S1 Expression of ChR2V in the brain of W-TChR2V4 rat.
(PDF)

Figure S2 Expression of ChR2V in the spinal cord and the motor nerve terminals.
(PDF)

Figure S3 Non-fluorescent DRG neurons were unresponsive to the blue light.
(PDF)

Figure S4 The primers that were used to differentiate ChR2V+ from ChR2V− rats.
(PDF)

Figure S5 Expression of ChR2V in the tail nerve bundles.
(PDF)

Acknowledgments

We wish to thank G. Nagel for the ChR2 cDNA, A. Miyawaki for the *Venus* cDNA, S. Hososhima, S. Inoue, D. Teh, A. Uchida, S. Watanabe and J. Yokose for experimental assistance, and B. Bell and D. Teh for language assistance.

Author Contributions

Conceived and designed the experiments: Z-GJ HY. Performed the experiments: Z-GJ SI TH HO. Analyzed the data: Z-GJ HY. Contributed reagents/materials/analysis tools: TI YF. Wrote the paper: Z-GJ HY.

References

1. Nathans J (1999) The evolution and physiology of human color vision: insights from molecular genetic studies of visual pigments. Neuron 24: 299–312.
2. Palczewski K (2006) G protein-coupled receptor rhodopsin. Annu Rev Biochem 75: 743–767.
3. Kaupp UB, Seifert R (2002) Cyclic nucleotide-gated ion channels. Physiol Rev 82: 769–824.
4. Bradley J, Reisert J, Frings S (2005) Regulation of cyclic nucleotide-gated channels. Curr Opin Neurobiol 15: 343–349.
5. Sineshchekov OA, Jung KH, Spudich JL (2002) Two rhodopsins mediate phototaxis to low and high intensity light in *Chlamydomonas reinhardtii*. Proc Natl Acad Sci U S A 99: 8689–8694.
6. Suzuki T, Yamasaki K, Fujita S, Oda K, Iseki M, et al. (2003) Archaeal-type rhodopsins in *Chlamydomonas*: model structure and intracellular localization. Biochem Biophys Res Commun 301: 711–717.
7. Kateriya S, Nagel G, Bamberg E, Hegemann P (2004) "Vision" in single-celled Algae. News Physiol, Sci 19: 133–137.
8. Nagel G, Ollig D, Fuhrmann M, Kateriya S, Musti AM, et al. (2002) Channelrhodopsin-1: a light-gated proton channel in green algae. Science 296: 2395–2398.
9. Nagel G, Szellas T, Huhn W, Kateriya S, Adeishvili N, et al. (2003) Channelrhodopsin-2, a directly light-gated cation-selective membrane channel. Proc Natl Acad Sci U S A 100: 13940–13945.
10. Hegemann P (2008) Algal sensory photoreceptors. Annu Rev Plant Biol 59: 167–189.
11. Boyden ES, Zhang F, Bamberg E, Nagel G, Deisseroth K (2005) Millisecond-timescale, genetically targeted optical control of neural activity. Nat Neurosci 8: 1263–1268.
12. Li X, Gutierrez DV, Hanson MG, Han J, Mark MD, et al. (2005) Fast noninvasive activation and inhibition of neural and network activity by vertebrate rhodopsin and green algae channelrhodopsin. Proc Natl Acad Sci U S A 102: 17816–17821.
13. Ishizuka T, Kakuda M, Araki R, Yawo H (2006) Kinetic evaluation of photosensitivity in genetically engineered neurons expressing green algae light-gated channels. Neurosci Res 54: 85–94.
14. Bi A, Cui J, Ma YP, Olshevskaya E, Pu M, et al. (2006) Ectopic expression of a microbial-type rhodopsin restores visual responses in mice with photoreceptor degeneration. Neuron 50: 23–33.
15. Tomita H, Sugano E, Yawo H, Ishizuka T, Isago H, et al. (2007) Restoration of visual response in aged dystrophic RCS rats using AAV-mediated channelopsin-2 gene transfer. Invest Ophthalmol Vis Sci 48: 3821–3826.
16. Tomita H, Sugano E, Fukazawa Y, Isago H, Sugiyama Y, et al. (2009) Visual properties of transgenic rats harboring the channelrhodopsin-2 gene regulated by the Thy-1.2 promoter. PLoS One 4: e7679.
17. Campagnola L, Wang H, Zylka MJ (2008) Fiber-coupled light-emitting diode for localized photostimulation of neurons expressing channelrhodopsin-2. J Neurosci Meth 169: 27–33.
18. Wang H, Zylka MJ (2009) *Mrgprd*-expressing polymodal nociceptive neurons innervate most known classes of substantia gelatinosa neurons. J Neurosci 29: 13202–13209.
19. Lawson SN, Waddell PJ (1991) Soma neurofilament immunoreactivity is related to cell size and fibre conduction velocity in rat primary sensory neurons. J Physiol 435: 41–63.
20. Julius D, Basbaum AI (2001) Molecular mechanisms of nociception. Nature 413: 203–210.
21. Celio MR (1990) Calbindin D-28k and parvalbumin in the rat nervous system. Neuroscience 35: 375–475.
22. Ichikawa H, Deguchi T, Nakago T, Jacobowitz DM, Sugimoto T (1994) Parvalbumin, calretinin and carbonic anhydrase in the trigeminal and spinal primary neurons of the rat. Brain Res 655: 241–245.
23. Basbaum AI, Jessell TM (2000) The perception of pain. In: Kandel ER, Schwartz JH, Jessell TM, eds. Principles of Neural Science Fourth Edition. New York: McGraw-Hill. pp 430–491.

24. Moll I, Roessler M, Brandner JM, Eispert AC, Houdek P, et al. (2005) Human merkel cells-aspects of cell biology, distribution and functions. Eur J Cell Biol 84: 259–271.
25. Kinnman E, Aldskogius H, Johansson O, Wiesenfeld-Hallin Z (1992) Collateral reinnervation and expansive regenerative reinnervation by sensory axons into "foreign" denervated skin: an immunohistochemical study in the rat. Exp Brain Res 91: 61–72.
26. Averill S, Mcmahon SB, Clary DO, Reichardt LF, Priestley JV (1995) Immunocytochemical localization of trkA receptors in chemically identified subgroups of adult rat sensory neurons. Eur J Neurosci 7: 1484–1494.
27. Snider WD, McMahon SB (1998) Tackling pain at the source: new ideas about nociceptors. Neuron 20: 629–632.
28. Zhang X, Bao L (2006) The development and modulation of nociceptive circuitry. Curr Opin Neurobiol 16: 460–466.
29. Ha SO, Yoo HJ, Park SY, Hong HS, Kim DS, et al. (2000) Capsaicin effects on brain-derived neurotrophic factor in rat dorsal root ganglia and spinal cord. Brain Res Mol Brain Res 81: 181–186.
30. Fang X, Djouhri L, McMullan S, Berry C, Waxman SG, et al. (2006) Intense isolectin-B4 binding in rat dorsal root ganglion neurons distinguishes C-fiber nociceptors with broad action potentials and high Nav1.9 expression. J Neurosci 26: 7281–7292.
31. Lu SG, Gold MS (2008) Inflammation-induced increase in evoked calcium transients in subpopulations of rat DRG neurons. Neuroscience 153: 279–288.
32. Dawson LF, Phillips JK, Finch PM, Inglis JJ, Drummond PD (2011) Expression of α_1-adrenoceptors on peripheral nociceptive neurons. Neuroscience 175: 300–314.
33. Vulchanova L, Riedl MS, Shuster SJ, Stone LS, Hargreaves KM, et al. (1998) $P2X_3$ is expressed by DRG neurons that terminate in inner lamina II. Eur J Neurosci 10: 3470–3478.
34. Novakovic SD, Kassotakis LC, Oglesby IB, Smith JA, Eglen RM, et al. (1999) Immunocytochemical localization of P2X3 purinoceptors in sensory neurons in naïve rats and following neuropathic injury. Pain 80: 273–282.
35. Caspary T, Anderson KV (2003) Patterning cell types in the dorsal spinal cord: what the mouse mutants say. Nat Rev Neurosci 4: 289–297.
36. Morris R, Cheunsuang O, Stewart A, Maxwell D (2004) Spinal dorsal horn neurone targets for nociceptive primary afferents: do single neurone morphological characteristics suggest how nociceptive information is processed at the spinal level. Brain Res Brain Res Rev 46: 173–190.
37. Coggeshall RE (2005) Fos, nociception and the dorsal horn. Prog Neurobiol 77: 299–352.
38. Todd AJ (2002) Anatomy of primary afferents and projection neurons in the rat spinal dorsal horn with particular emphasis on substance P and the neurokinin 1 receptor. Exp Physiol 87: 245–249.
39. Provitera V, Nolano M, Pagano A, Caporaso G, Stancanelli A, et al. (2007) Myelinated nerve endings in human skin. Muscle Nerve 35: 767–775.
40. Perry MJ, Lawson SN, Robertson J (1991) Neurofilament immunoractivity in populations of rat primary afferent neurons: a quantitative study of phosphorylated and non-phosphorylated subunits. J Neurocytol 20: 746–758.
41. Melean MJ, Bennett PB, Thomas RM (1988) Subtypes of dorsal root ganglion neurons based on different inward currents as measured by whole-cell voltage clamp. Mol Cell Biochem 80: 95–107.
42. Villière V, McLachlan EM (1996) Electrophysiological properties of neurons in intact rat dorsal root ganglia classified by conduction velocity and action potential duration. J Neurophysiol 76: 1924–1941.
43. Price MP, Lewin GR, McIlwrath SL, Cheng C, Xie J, et al. (2000) The mammalian sodium channel BNC1 is required for normal touch sensation. Nature 407: 1007–1011.
44. Tan ZY, Donnelly DF, LaMotte RH (2006) Effects of a chronic compression of the dorsal root ganglion on voltage-gated Na^+ and K^+ currents in cutaneous afferent neurons. J Neurophysiol 95: 1115–1123.
45. Hu J, Chiang LY, Koch M, Lewin GR (2010) Evidence for a protein tether involved in somatic touch. EMBO J 29: 855–867.
46. Tamamaki N, Nakamura K, Furuta T, Asamoto K, Kaneko T (2000) Neurons in Golgi-stain-like images revealed by GFP-adenovirus infection in vivo. Neurosci Res 38: 231–236.
47. Gong S, Zheng C, Doughty ML, Losos K, Didkovsky N, et al. (2003) A gene expression atlas of the central nervous system based on bacterial artificial chromosomes. Nature 425: 917–925.
48. Torsney C, Anderson RL, Ryce-Paul KA, MacDermott AB (2006) Characterization of sensory neuron subpopulations selectively expressing green fluorescent protein in phosphodiesterase 1C BAC transgenic mice. Mol Pain 2: 17.
49. Hu HZ, Li ZW (1997) Modulation by adenosine of GABA-activated current in rat dorsal root ganglion neurons. J Physiol 501: 67–75.

J Mol Neurosci (2012) 46:393–400
DOI 10.1007/s12031-011-9599-y

Age-Dependent Differences in Recovered Visual Responses in Royal College of Surgeons Rats Transduced with the Channelrhodopsin-2 Gene

Hitomi Isago · Eriko Sugano · Zhuo Wang · Namie Murayama · Eri Koyanagi · Makoto Tamai · Hiroshi Tomita

Received: 29 November 2010 / Accepted: 12 July 2011 / Published online: 27 July 2011

Abstract The objective of this study is to investigate age-related differences in recovered visual function in Royal College of Surgeons (RCS) rats transduced with the Channelrhodopsin-2 (ChR2) gene. An adeno-associated virus vector that contained *ChR2* was injected intravitreously into young or aged RCS rats. After 4 months, visual evoked potentials were recorded. To estimate the transduction efficiencies, ChR2V-expressing cells and retrograde labeled retinal ganglion cells (RGCs) were counted. After photoreceptor degradation, immunohistochemistry was used to detect glial fibrillary acidic protein (GFAP) in the retinas. The amplitudes and latencies from young RCS rats were higher and shorter, respectively, than those from aged RCS rats. ChR2V was expressed in the RGCs of both groups of rats; there was no significant difference in the transduction efficiency of either group. However, the number of RGCs in aged RCS rats was significantly less than that in young RCS rats. In addition, strong GFAP immunoreactivity was observed after photoreceptor degeneration, whereas it was weaker in ChR2V-expressing RGCs. *ChR2* transduction produced photosensitive RGCs in both young and aged rats. However, the degree of recovery depended on the age at the time of transduction.

Keywords Channelrhodopsin-2 · Adeno-associated virus vector · Royal College of Surgeons rat · Visual evoked potentials

H. Isago · E. Sugano · Z. Wang · N. Murayama · E. Koyanagi · H. Tomita (✉)
Institute for International Advanced Interdisciplinary Research, Tohoku University,
4-1 Seiryo-machi, Aoba-ku,
Sendai 980-8575, Japan
e-mail: hiroshi-tomita@iiare.tohoku.ac.jp

H. Tomita
Tohoku University School of Medicine United Centers for Advanced Research and Translational Medicine,
Sendai, Japan

H. Tomita
Tohoku University Hospital Innovation of New Biomedical Engineering Center,
Sendai, Japan

M. Tamai
Tohoku University Graduate School of Medicine,
Sendai, Japan

Z. Wang
Japan Foundation for Aging and Health,
Sendai, Japan

Introduction

Channelrhodopsin-2 (ChR2) (Nagel et al. 2003; Sineshchekov et al. 2002) is a 7-transmembrane protein that contains an all-*trans*-retinal chromophore(Tsuda et al. 1980) and functions as a light-driven cation-selective channel (Nagel et al. 2003). Since *ChR2* transduction can confer photosensitivity to neurons (Boyden et al. 2005; Ishizuka et al. 2006), channelrhodopsins have optogenetic applications to restore vision.

Retinitis pigmentosa (RP), the common inherited disease that causes blindness, has a prevalence of 1 in 4,000. Although RP is considered to be an incurable disease because photoreceptor cells are often degenerated, other retinal neurons, such as retinal ganglion cells (RGCs), that

are usually preserved can be used to restore vision (Humayun et al. 1999; Santos et al. 1997; Stone et al. 1992). For example, Bi et al. (2006) showed that transducing *ChR2* into RGCs restores the visual responses in the rd1 mouse model of RP (Bowes et al. 1990; McLaughlin et al. 1993). Similarly, we restored visual (Tomita et al. 2007) and behavioral responses (Tomita et al. 2010) in another type of genetically blind rats, Royal College of Surgeons rats and photoreceptor-degenerated Thy-I ChR2 transgenic rats (Tomita et al. 2009). Thus, *ChR2* gene therapy is a potentially promising treatment for RP patients with viable RGCs. The number of remaining RGCs depends on the disease progression. In severe cases, they may be eliminated (Humayun et al. 1999). In general, functional abnormalities of the inner retinal neurons and retinal remodeling occur after photoreceptor degeneration (Strettoi et al. 2002, 2003). However, the function of RGCs after photoreceptor degeneration is not completely understood.

To elucidate the age dependence of the function of the remaining RGCs after photoreceptor degeneration, we transduced *ChR2* into the RGCs of young and aged RCS rats and then measured their electrophysiological functions.

Materials and Methods

Animals

Young (6-month-old) and aged (10-month-old) male RCS (rdy/rdy) rats were purchased from CLEA Japan, Inc. These rats were maintained on a 12-h light–dark cycle and fed standard laboratory chow and water ad libitum. All experiments were approved by the Animal Research Committee, Graduate School of Medicine, Tohoku University, Japan. In addition, the experimental procedures adhered to the Association for Research in Vision and Ophthalmology Statement for the Use of Animals in Ophthalmologic and Vision Research.

Preparation of the Adeno-Associated Virus Vector

The adeno-associated virus (AAV) vector with the ChR2 gene was constructed as described previously (Tomita et al. 2007). Briefly, the first 315 amino acids of ChR2 (GenBank Accession No. AF461397) were fused to Venus, a fluorescent protein. Then, the AAV Helper-Free System (Stratagene, La Jolla, CA) was used to produce infectious, AAV-Venus (control) and AAV-ChR2V virions, which were purified by a single-step column purification method as previously described (Sugano et al. 2005).

Intravitreal Delivery of Adeno-Associated Virus

The AAVs were injected into rats at the times shown in Fig. 1. Prior to this operation, the rats were anesthetized by an intramuscular injection of 66 mg kg^{-1} ketamine and 33 mg kg^{-1} xylazine. Then, by using an operating microscope, an incision was made into the conjunctiva to expose the sclera. Five microliters of a suspension that contained $1–10\times10^{12}$ virions·μL^{-1} was intravitreally injected through the ora serrata with a 10-μL Hamilton syringe with a 32-G needle (Hamilton Company, Reno,

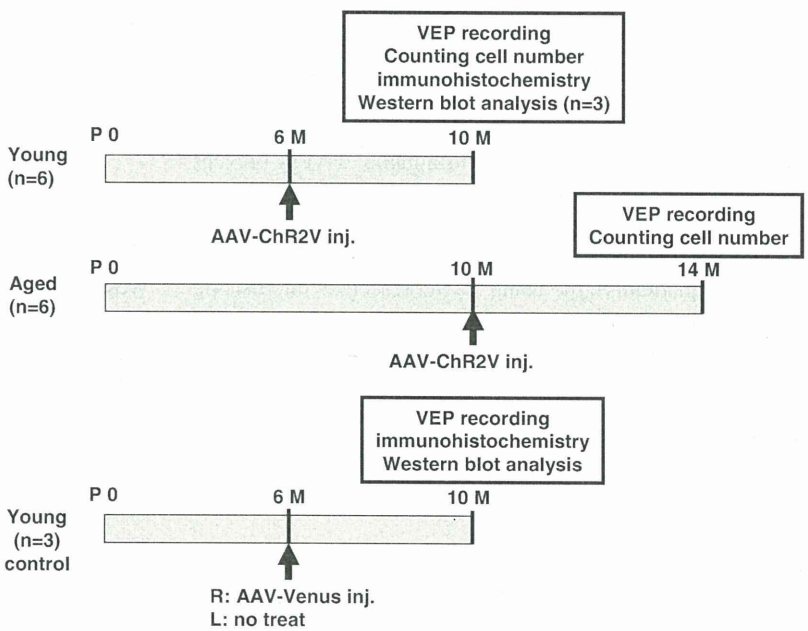

Fig. 1 Experimental design. Adeno-associated virus vectors that contained the Channelrhodopsin-2 gene (AAV-ChR2V) were injected intravitreally into 6- or 10-month-old Royal College of Surgeons (RCS) rats. After recording visual evoked potentials (VEPs), the left (*L*) eyes were used for cell counts and immunohistochemistry. As a control, AAV vectors that contained the gene for the Venus fluorescent protein (AAV-Venus) were injected into the right (*R*) eye of 6-month-old RCS rats

NV). The AAV-ChR2V virions were injected into both eyes of young and aged RCS rats. As a control, the AAV-Venus virions were injected into the right eye of young RCS rats.

Recording of Visual Evoked Potentials

Four months after the intravitreous injections, the visual evoked potentials (VEPs) were recorded as described previously (Tomita et al. 2007, 2009, 2010). Briefly, VEPs were recorded by using a Neuropack (MEB-9102; Nihon Kohden, Tokyo, Japan). First, the rats were anaesthetized with ketamine-xylazine, and then their pupils were dilated with 1% atropine and 2.5% phenylephrine hydrochloride. Photic stimuli of various intensities were generated from a blue light-emitting diode (LED) at 435–500 nm (peak at 470 nm) and applied for 10 ms with a frequency of 0.5 Hz. The high and low pass filters were set to 50 and 0.05 kHz, respectively. VEP responses were measured 100 consecutive times, and then the response waveform was averaged.

Retrograde Labeling of Retinal Ganglion Cells

After recording the VEPs, retrograde labeling was used to identify RGCs in the ganglion cell layer. The labeling was performed by injecting 4 μL of a solution of 2% aqueous fluorogold (FG; Fluorochrome, Englewood, CO) (Brecha and Weigmann 1994) and 1% dimethylsulfoxide into the superior colliculus with a Hamilton syringe and a 32-G needle (Sato et al. 2005).

Determination of Transduction Efficiency

At the end of the experiment, the rats were sacrificed and their eyes were resected and fixed in 4% paraformaldehyde and 0.1 M phosphate buffer, pH 7.4. The left eye of each rat was flat-mounted on a slide and covered with Vectashield medium (Vector Laboratories, Burlingame, CA) to prevent the degradation of fluorescence. Then, the number of fluorogold-positive RGCs and double-positive (fluorogold and Venus) RGCs were counted in 12 different areas (3 areas×4 quadrants) by using a fluorescence microscope (Axiovert 40, Carl Zeiss, Tokyo). These numbers were used to estimate the transduction efficiency of AAV-ChR2V. In addition, the vertical image in the retinal whole mount was reconstructed from z-stacked images that were captured with the Apotome® z-scanning mode of the Axiovert 40 microscope.

Immunohistochemistry

The right eye of each rat was rinsed with phosphate-buffered saline (PBS) and serially immersed in 10%, 20%, and 30% sucrose in PBS at 4°C. Subsequently, the samples were embedded in optimal cutting temperature compound (Sakura, Tokyo, Japan), and then stored at −80°C (Tomita et al. 2005). Tissue cryosections (10 μm thick) were mounted on slides and air-dried. These sections were incubated with blocking buffer (0.05% Tween-20, 3% BSA, 3% goat serum in PBS) at room temperature (RT) for 1 h, and then with mouse anti-rat glial fibrillary acid protein (GFAP) antibody (1:250; Nihon Millipore, Tokyo, Japan) with blocking buffer overnight at 4°C. For the negative control, sections were incubated with the same concentration of mouse immunoglobulin G (IgG). After the incubations, the sections were rinsed three times with PBS, incubated with Alexa 594-conjugated anti-mouse IgG antibody (Molecular Probes, Eugene, OR) at RT for 30 min, and then rinsed three times with PBS. Finally, the sections were mounted with Vectashield medium (Vector Laboratories, Burlingame, CA), and the GFAP immunoreactivity was visualized with an Axiovert40 fluorescence microscope.

Antibody Production

A polyclonal antibody was prepared against the ChR2. Two Japanese white rabbits were injected intradermally with 200 μg of the synthetic peptides GDIRKTTKLNIGGT (279–292aa), emulsified with complete Freund's adjuvant. Keyhole limpet hemocyanin (KLH) was used as a carrier protein, and synthetic peptides were conjugated to it by the *m*-maleimidobenzoyl-*N*-hydroxysuccinimide ester method. The rabbits received five booster injections of the synthetic peptide emulsified with incomplete Freund's adjuvant. Following the measurement of the antibody titer by ELISA, whole blood was collected and then the serum was purified through a KLH column.

Western Blot Analysis

Retinas were lysed and sonicated in lysis buffer [10 mM Tris–HCl, 0.5% *n*-Dodecyl-β-D-maltoside, pH 8.0 containing a protease inhibitor (Roche Diagnostics, Tokyo)]. For Western blots of GFAP, ChR2, and β-actin in the retinal extracts (12 μg protein) were electrophoresed on 4–20% SDS–polyacrylamide gels (BIO-RAD, Tokyo) and transferred onto a PVDF membrane. The membranes were bathed with the GFAP antibody and then washed three times with TBST [10 mM Tris–HCl (pH 8.0), 150 mM NaCl, and 0.1% Tween 20]. Alkaline phosphatase-conjugated goat anti-mouse IgG (Invitrogen, Tokyo) was used as secondary antibody. Protein bands were developed by the CDP-star detection reagent (GE Healthcare, Tokyo) according to the manufacturer's instructions. Protein bands were detected by exposing the membranes to X-ray film

(Fuji, Tokyo, Japan). The membranes were then stripped of the first antibody and reprobed with antibodies of β-actin (Santa Cruz Biotechnology, Santa Cruz, CA) or ChR2.

Statistical Analysis

Statistical analysis was performed by using GraphPad Prism software ver. 4.00 (GraphPad Software, San Diego, CA). Statistically significant differences were determined by using unpaired t tests. The criterion for statistical significance was $p<0.05$.

Results

Visual Evoked Potentials

No VEPs were recorded in any of the wild-type or control RCS rats, even with most intense photic stimuli (data not shown). In contrast, photic stimuli produced VEPs in both the young and aged RCS rats that were infected with the AAV-ChR2V virions. However, there were some differences between the overall shapes of the waveforms of the young and aged RCS rats (Fig. 2a). For example, the VEP amplitudes from young RCS rats were larger than those from aged RCS rats (Fig. 2b). In addition, the P1 latency in young RCS rats was significantly shorter than that in aged RCS rats (Fig. 2c).

Transduction Efficiency of ChR2V

ChR2V was expressed in the retinas of both young (Fig. 3a) and aged RCS rats (Fig. 3b). Most ChR2V-expressing cells were considered to be RGCs because their axons and dendrites were labeled with Venus fluorescent protein. In addition, a vertical section of the z-stacked images showed that the ChR2V-expressing cells coincided with retrograde-labeled RGCs (Fig. 3c). The number of RGCs and double-labeled RGCs in the retinas of aged rats was less than that of young rats (Fig. 3d). However, the transduction efficiencies in the retinas of young (28.3±5.3%) and aged (27.7±9.5%) rats were very similar.

Immunohistochemistry and Western Blot Analysis

GFAP immunoreactivity was strong after photoreceptor degeneration (Fig. 4a–c). However, GFAP immunoreactivity was weak in ChR2V-expressing retinal cells (Fig. 4d). Western blot analysis of retinal extracts showed that the GFAP protein expression in untreated or AAV-Venus injected RCS rats was higher than that in AAV-ChR2V injected RCS

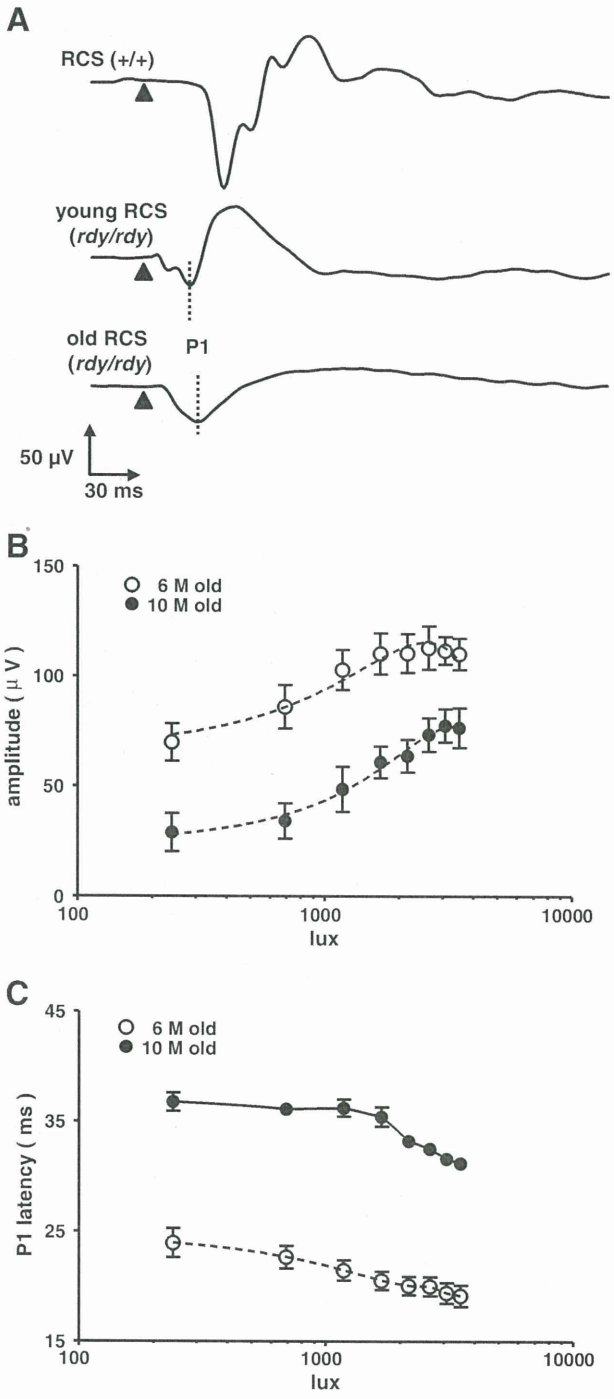

Fig. 2 VEPs recorded from the eyes of young and aged RCS rats transduced with the Channelrhodopsin-2 (ChR2) gene. **a** Typical waveforms evoked by photic stimuli from a blue LED (*upper panel*: wild-type rat, *middle panel*: young RCS rat, *lower panel*: aged RCS rat). **b**, **c** The relationships between the light stimulus intensity and VEP amplitude (**b**) or the P1 latency (**c**). The *data points and error bars* indicate the mean and standard deviation, respectively ($n=6$)

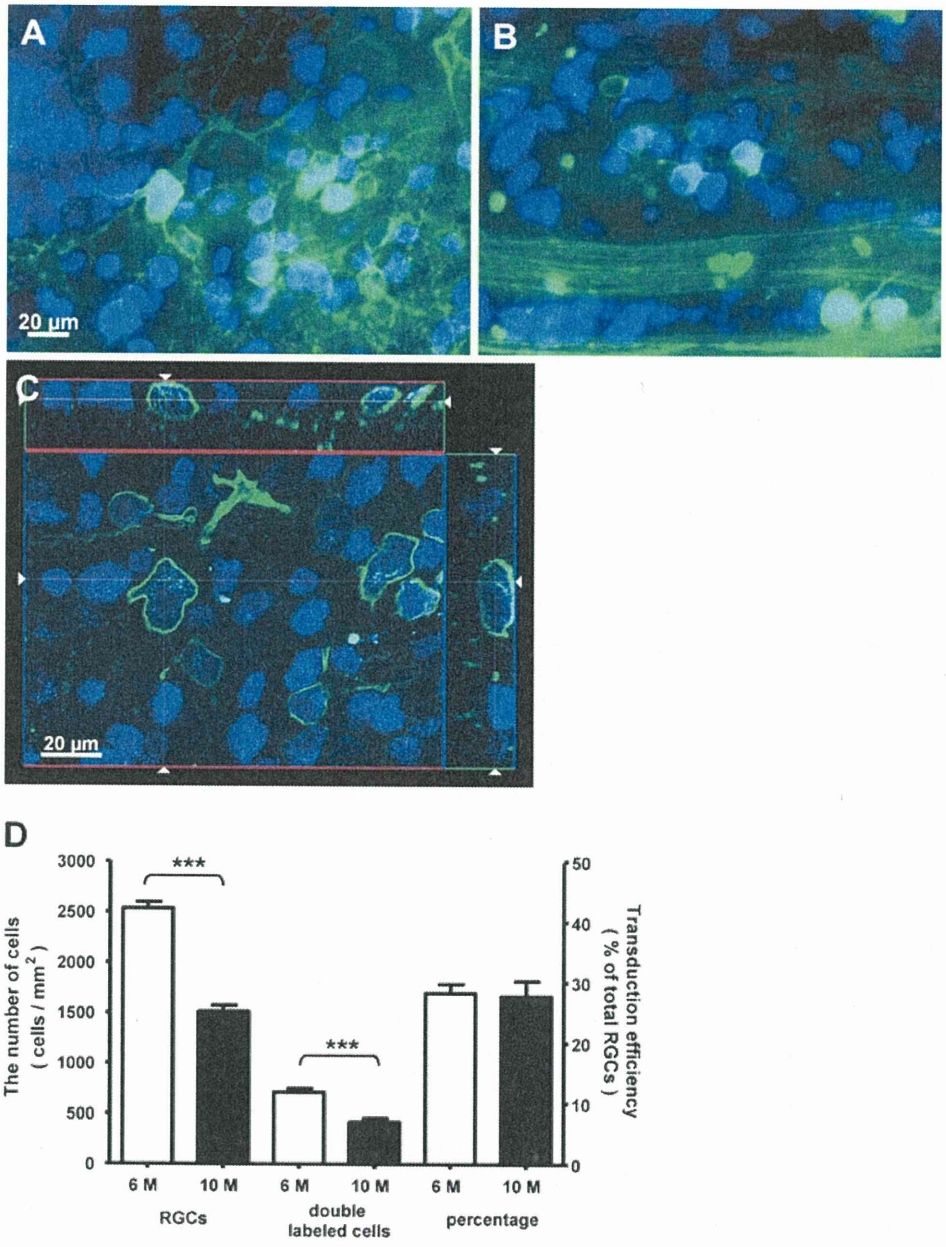

Fig. 3 ChR2V expression in the inner retinal layers of the eyes of young and aged RCS rats. **a**, **b** Fluorescence microphotographs from young (**a**) and aged (**b**) RCS rats. **c** A vertical image of the retina in a young RCS rat that was reconstructed from z-stacked images. **d** The transduction efficiencies were estimated by counting Venus and fluorogold positive cells. The *height of the bars* and the *error bars* indicate the mean and standard deviation, respectively (n=6). ***p<0.001

rats. The GFAP protein expression was slightly detected in non-dystrophic (RCS, +/+) rats (Fig. 4e).

Discussion

Degenerative eye diseases, such as RP, usually affect photoreceptor cells first. Subsequently, RGCs are also affected and the inner retinal neurons are remodeled (Grunder et al. 2001; Marc et al. 2003, 2007; Strettoi and Pignatelli 2000; Strettoi et al. 2002, 2003). However, the function of the remaining RGCs is not clear. In this study, we observed age-dependent reductions in the number of RGCs. In addition, the ChR2V-expressing RGCs of both young and aged rats responded to light stimuli and evoked potentials. Although there were some differences in the maximum VEP amplitudes in the two groups of rats, they both showed similar increases in VEP amplitude with increasing stimulus intensity. These results indicated that the surviving RGCs are still able to produce action potentials.

Histological examinations show that photoreceptor degeneration in RCS rats begins on approximately

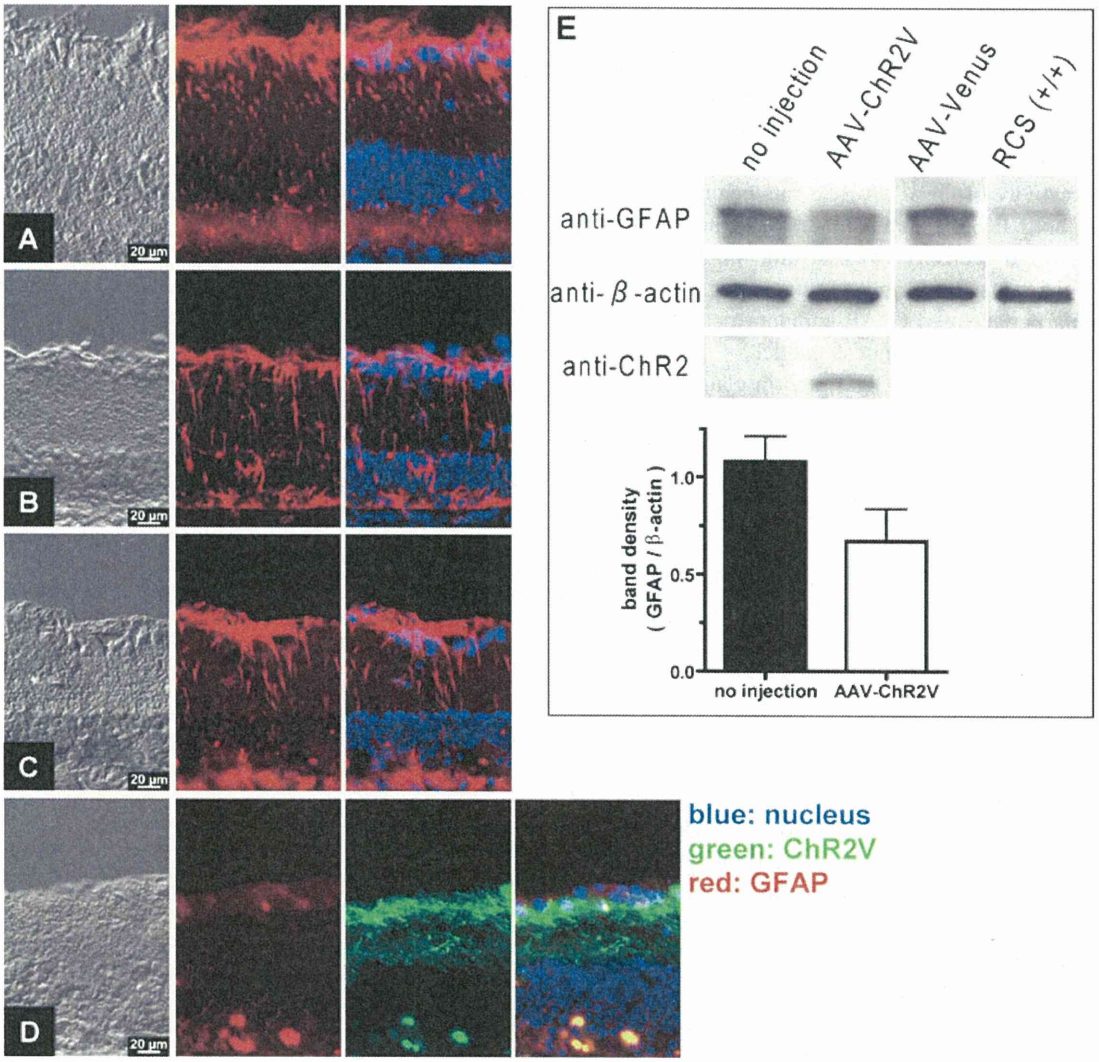

Fig. 4 Changes in GFAP immunoreactivity after photoreceptor degeneration. GFAP immunoreactivity (*red*) was measured in 3-month-old (**a**), 6-month-old (**b**), and 10-month-old (**c**) RCS rats. **d** Weak GFAP immunoreactivity was observed in the retinal cells of young RCS rats that had been transduced with Ch2R. Western blots showed the decreased GFAP protein expression in AAV-ChR2V transduced rat retinas (**e**)

postnatal day 20 (P20) and ends with rod degeneration by P100 (LaVail and Battelle 1975; Mullen and LaVail 1976; Tamai and Chader 1979). Similarly, electroretinogram analyses demonstrate that photoreceptors disappear by P80 (Bush et al. 1995; Sauve et al. 2004). In the latter studies, the first definitive signs of photoreceptor degeneration are decreased receptive field size, contrast sensitivity, and threshold sensitivity within a month after birth (Pu et al. 2006). However, these characteristics are determined by indirect stimulation of RGCs by photoreceptors because the native RGCs are not light sensitive. In this study, we overcame this limitation by transducing RGCs with *ChR2* to make them photosensitive.

We did not observe a decrease in the number of RGCs in young RCS rats, which is consistent with a previous study that did not show any significant loss of RGCs for 6 months (Pavlidis et al. 2000). In contrast, we observed a significant loss of RGCs in aged RCS rats. Interestingly, the transduction efficiencies of both groups of rats were the same; however, the cause is not known. Since RGCs are classified into different groups by their morphology (Huxlin and Goodchild 1997), it is possible that the AAV type-2 vector may have a higher affinity to some types of RGCs. Nevertheless, the high transduction efficiency of the AAV type-2 vector in RGCs in this study is in agreement with previous results (Ali et al. 1998; Martin et al. 2002). The lack of a significant difference between the contribution of individual ChR2-expressing RGCs to the maximum VEP amplitude in young and aged RCS rats (young rats: 111.7±17.7 μV/710.6±117.7 cells=0.157 $\mu V \cdot cell^{-1}$, aged rats: 77.5±15.1 μV/414.2±144.5 cells=0.187 $\mu V \cdot cell^{-1}$) indicated that the activity of individual RGCs was independent of age.

Since GFAP is expressed as a result of gliosis and hypertrophy of macroglial cells, it is a common marker of pathological or stressful conditions in astrocytes and Müller cells in the retina (Hartig et al. 1995; Reichenbach and Reichelt 1986). Kimura et al. (2000) showed that the immunoreactivity of GFAP in RCS rats begins at P35 and continues until P105. In this study, we demonstrated that GFAP immunoreactivity was strong in Müller cells 3 months after the birth and continued for more than a year. Similarly, increased GFAP immunoreactivity also has been observed in the rd mouse model of photoreceptor degeneration (Strettoi et al. 2003) and in glaucoma models that caused the death of RGCs (Schuettauf et al. 2004; Tezel et al. 2003). The increased immunoreactivity might be due to stress responses that are associated with the degeneration of photoreceptors, second order neurons, or Müller cells. We observed decreased GFAP immunoreactivity in ChR2V-expressing RGCs. Dai et al. (2011) recently reported that GFAP protein expression increased in Müller cells during the death of RGCs caused by the experimental glaucoma model and the GFAP expression was inhibited by the rescue of RGCs death. The activation of astroglia or Müller cells coincides with the degeneration of RGCs (Bosco et al. 2008; Schmidt et al. 2007; Schuettauf et al. 2004; Tezel et al. 2003). Taken together with our previous report that VEPs could be maintained for up to 64 weeks after the *ChR2* transduction (Sugano et al. 2010; Tomita et al. 2010), ChR2V may inhibit secondary degeneration of RGCs in the retina. Although the mechanism of this protection is not known, ChR2V may stimulate RGCs or neurotrophic factors. For example, it is known that electrical stimulation of the retina prevents secondary degeneration (Schmid et al. 2009) and axotomy-induced RGC death (Morimoto et al. 2002, 2005, 2010). Similarly, depolarization and elevation of intracellular cAMP in RGCs increase the levels of brain-derived neurotrophic factor (BDNF) receptor trkB, which prevents RGC cell death because BDNF acts as a survival factor for RGCs (Meyer-Franke et al. 1998; Shen et al. 1999) Further study is needed to elucidate the mechanism of the antidegenerative effects of ChR2.

In conclusion, our results showed that although the number of RGCs decreased during photoreceptor degeneration, the activity of individual RGCs was preserved. In addition, *ChR2* transduction can produce photosensitive RGCs in both young and aged rats. However, the degree of recovery depended on their age at the time of transduction.

Grant support This work was partly supported by Grants-in-Aid for Scientific Research from the Ministry of Education, Culture, Sports, Science and Technology of Japan (No. 21791664 and 21200022); Science and Culture and Special Coordination Funds for Promoting Science and Technology of the Japanese Government, Strategic Research Program for Brain Sciences (SRPBS); Ministry of Health, Labour and Welfare of Japan; Japan Foundation for Aging and Health; and the Program for Promotion of Fundamental Studies in Health Sciences of the National Institute of Biomedical Innovation (NIBIO).

References

Ali RR, Reichel MB, De Alwis M et al (1998) Adeno-associated virus gene transfer to mouse retina. Hum Gene Ther 9:81–86

Bi A, Cui J, Ma YP et al (2006) Ectopic expression of a microbial-type rhodopsin restores visual responses in mice with photoreceptor degeneration. Neuron 50:23–33

Bosco A, Inman DM, Steele MR et al (2008) Reduced retina microglial activation and improved optic nerve integrity with minocycline treatment in the DBA/2J mouse model of glaucoma. Invest Ophthalmol Vis Sci 49:1437–1446

Bowes C, Li T, Danciger M, Baxter LC, Applebury ML, Farber DB (1990) Retinal degeneration in the rd mouse is caused by a defect in the beta subunit of rod cGMP-phosphodiesterase. Nature 347:677–680

Boyden ES, Zhang F, Bamberg E, Nagel G, Deisseroth K (2005) Millisecond-timescale, genetically targeted optical control of neural activity. Nat Neurosci 8:1263–1268

Brecha NC, Weigmann C (1994) Expression of GAT-1, a high-affinity gamma-aminobutyric acid plasma membrane transporter in the rat retina. J Comp Neurol 345:602–611

Bush RA, Hawks KW, Sieving PA (1995) Preservation of inner retinal responses in the aged Royal College of Surgeons rat. Evidence against glutamate excitotoxicity in photoreceptor degeneration. Invest Ophthalmol Vis Sci 36:2054–2062

Dai Y, Weinreb RN, Kim KY et al (2011) Inducible nitric oxide synthase-mediated alteration of mitochondrial OPA1 expression in ocular hypertensive rats. Invest Ophthalmol Vis Sci 52:2468–2476

Grunder T, Kohler K, Guenther E (2001) Alterations in NMDA receptor expression during retinal degeneration in the RCS rat. Vis Neurosci 18:781–787

Hartig W, Grosche J, Distler C, Grimm D, El-Hifnawi E, Reichenbach A (1995) Alterations of Muller (glial) cells in dystrophic retinae of RCS rats. J Neurocytol 24:507–517

Humayun MS, Prince M, de Juan E Jr et al (1999) Morphometric analysis of the extramacular retina from postmortem eyes with retinitis pigmentosa. Invest Ophthalmol Vis Sci 40:143–148

Huxlin KR, Goodchild AK (1997) Retinal ganglion cells in the albino rat: revised morphological classification. J Comp Neurol 385:309–323

Ishizuka T, Kakuda M, Araki R, Yawo H (2006) Kinetic evaluation of photosensitivity in genetically engineered neurons expressing green algae light-gated channels. Neurosci Res 54:85–94

Kimura N, Nishikawa S, Tamai M (2000) Muller cells in developing rats with inherited retinal dystrophy. Tohoku J Exp Med 191:157–166

LaVail MM, Battelle BA (1975) Influence of eye pigmentation and light deprivation on inherited retinal dystrophy in the rat. Exp Eye Res 21:167–192

Marc RE, Jones BW, Watt CB, Strettoi E (2003) Neural remodeling in retinal degeneration. Prog Retin Eye Res 22:607–655

Marc RE, Jones BW, Anderson JR et al (2007) Neural reprogramming in retinal degeneration. Invest Ophthalmol Vis Sci 48:3364–3371

Martin KR, Klein RL, Quigley HA (2002) Gene delivery to the eye using adeno-associated viral vectors. Methods 28:267–275

McLaughlin ME, Sandberg MA, Berson EL, Dryja TP (1993) Recessive mutations in the gene encoding the beta-subunit of rod phosphodiesterase in patients with retinitis pigmentosa. Nat Genet 4:130–134

Meyer-Franke A, Wilkinson GA, Kruttgen A et al (1998) Depolarization and cAMP elevation rapidly recruit TrkB to the plasma membrane of CNS neurons. Neuron 21:681–693

Morimoto T, Miyoshi T, Fujikado T, Tano Y, Fukuda Y (2002) Electrical stimulation enhances the survival of axotomized retinal ganglion cells in vivo. Neuroreport 13:227–230

Morimoto T, Miyoshi T, Matsuda S, Tano Y, Fujikado T, Fukuda Y (2005) Transcorneal electrical stimulation rescues axotomized retinal ganglion cells by activating endogenous retinal IGF-1 system. Invest Ophthalmol Vis Sci 46:2147–2155

Morimoto T, Miyoshi T, Sawai H, Fujikado T (2010) Optimal parameters of transcorneal electrical stimulation (TES) to be neuroprotective of axotomized RGCs in adult rats. Exp Eye Res 90:285–291

Mullen RJ, LaVail MM (1976) Inherited retinal dystrophy: primary defect in pigment epithelium determined with experimental rat chimeras. Science 192:799–801

Nagel G, Szellas T, Huhn W et al (2003) Channelrhodopsin-2, a directly light-gated cation-selective membrane channel. Proc Natl Acad Sci USA 100:13940–13945

Pavlidis M, Fischer D, Thanos S (2000) Photoreceptor degeneration in the RCS rat attenuates dendritic transport and axonal regeneration of ganglion cells. Invest Ophthalmol Vis Sci 41:2318–2328

Pu M, Xu L, Zhang H (2006) Visual response properties of retinal ganglion cells in the royal college of surgeons dystrophic rat. Invest Ophthalmol Vis Sci 47:3579–3585

Reichenbach A, Reichelt W (1986) Postnatal development of radial glial (Muller) cells of the rabbit retina. Neurosci Lett 71:125–130

Santos A, Humayun MS, de Juan E Jr et al (1997) Preservation of the inner retina in retinitis pigmentosa. A morphometric analysis. Arch Ophthalmol 115:511–515

Sato H, Tomita H, Nakazawa T, Wakana S, Tamai M (2005) Deleted in polyposis 1-like 1 gene (Dp111): a novel gene richly expressed in retinal ganglion cells. Invest Ophthalmol Vis Sci 46:791–796

Sauve Y, Lu B, Lund RD (2004) The relationship between full field electroretinogram and perimetry-like visual thresholds in RCS rats during photoreceptor degeneration and rescue by cell transplants. Vision Res 44:9–18

Schmid H, Herrmann T, Kohler K, Stett A (2009) Neuroprotective effect of transretinal electrical stimulation on neurons in the inner nuclear layer of the degenerated retina. Brain Res Bull 79:15–25

Schmidt JF, Agapova OA, Yang P, Kaufman PL, Hernandez MR (2007) Expression of ephrinB1 and its receptor in glaucomatous optic neuropathy. Br J Ophthalmol 91:1219–1224

Schuettauf F, Rejdak R, Walski M et al (2004) Retinal neurodegeneration in the DBA/2J mouse-a model for ocular hypertension. Acta Neuropathol 107:352–358

Shen S, Wiemelt AP, McMorris FA, Barres BA (1999) Retinal ganglion cells lose trophic responsiveness after axotomy. Neuron 23:285–295

Sineshchekov OA, Jung KH, Spudich JL (2002) Two rhodopsins mediate phototaxis to low- and high-intensity light in Chlamydomonas reinhardtii. Proc Natl Acad Sci USA 99:8689–8694

Stone JL, Barlow WE, Humayun MS, de Juan E Jr, Milam AH (1992) Morphometric analysis of macular photoreceptors and ganglion cells in retinas with retinitis pigmentosa. Arch Ophthalmol 110:1634–1639

Strettoi E, Pignatelli V (2000) Modifications of retinal neurons in a mouse model of retinitis pigmentosa. Proc Natl Acad Sci USA 97:11020–11025

Strettoi E, Porciatti V, Falsini B, Pignatelli V, Rossi C (2002) Morphological and functional abnormalities in the inner retina of the rd/rd mouse. J Neurosci 22:5492–5504

Strettoi E, Pignatelli V, Rossi C, Porciatti V, Falsini B (2003) Remodeling of second-order neurons in the retina of rd/rd mutant mice. Vision Res 43:867–877

Sugano E, Tomita H, Ishiguro S, Abe T, Tamai M (2005) Establishment of effective methods for transducing genes into iris pigment epithelial cells by using adeno-associated virus type 2. Invest Ophthalmol Vis Sci 46:3341–3348

Sugano E, Isago H, Wang Z, Hiroi T, Tamai M, Tomita H (2010) Immune responses to adeno-associated virus type 2 encoding channelrhodopsin-2 in a genetically blind rat model for gene therapy. Gene Therapy 18:266–274

Tamai M, Chader GJ (1979) The early appearance of disc shedding in the rat retina. Invest Ophthalmol Vis Sci 18:913–917

Tezel G, Chauhan BC, LeBlanc RP, Wax MB (2003) Immunohistochemical assessment of the glial mitogen-activated protein kinase activation in glaucoma. Invest Ophthalmol Vis Sci 44:3025–3033

Tomita H, Kotake Y, Anderson RE (2005) Mechanism of protection from light-induced retinal degeneration by the synthetic antioxidant phenyl-N-tert-butylnitrone. Invest Ophthalmol Vis Sci 46:427–434

Tomita H, Sugano E, Yawo H et al (2007) Restoration of visual response in aged dystrophic RCS rats using AAV-mediated channelopsin-2 gene transfer. Invest Ophthalmol Vis Sci 48:3821–3826

Tomita H, Sugano E, Fukazawa Y et al (2009) Visual properties of transgenic rats harboring the channelrhodopsin-2 gene regulated by the thy-1.2 promoter. PLoS One 4:e7679

Tomita H, Sugano E, Isago H et al (2010) Channelrhodopsin-2 gene transduced into retinal ganglion cells restores functional vision in genetically blind rats. Exp Eye Res 90:429–436

Tsuda M, Glaccum M, Nelson B, Ebrey TG (1980) Light isomerizes the chromophore of bacteriorhodopsin. Nature 287:351–353

東北大グループ
緑藻遺伝子で視力再生
目に注入、ラットで成功

クラミドモナスという光を感知できる緑藻の遺伝子を目に注入することにより、特定の疾病で失明した場合は正常時とほぼ同じ視力を回復することが東北大国際高等融合領域研究所の富田浩史准教授（分子生物学）と菅野江里子助教（細胞工学）らの研究で分かった。ラットを使った実験での効果だが、この遺伝子治療を人間に応用して実用化できれば失明の治療につながると期待される。

中途失明者のうち遺伝性の網膜色素変性症や、近年高齢者に増加している加齢黄斑（こうはん）変性症が失明原因の上位を占める。必ず失明に至るとは限らないが、有効な治療法はないという。

これらの疾病で失明した場合、網膜にある光を受け取る視細胞は機能しなくなる。ただ脳に情報を伝える役割を担う網膜の神経節細胞は、正常な状態で残っていることが分かっている。

研究グループはこの点に着目。失明させたラットの実験で、神経節細胞に緑藻の遺伝子を注入して視細胞の機能を新たに与えることに成功した。

さらに視覚の回復程度も検証。緑藻の遺伝子を持つラットの場合、視細胞を壊しても神経節細胞がその機能を代替し、正常な状態と同程度の視力を持つことを証明した。また明暗の差を見分ける能力は正常時よりも高くなった。

ただ緑藻の遺伝子は青色しか感知できないなどの課題もある。今後、サルなどでも検証を重ねた上で臨床試験実施を目指す。

網膜色素・加齢黄斑変性
失明治療に道

厚生労働省などによると、網膜色素変性症の患者は国内で約2万5000人、加齢黄斑変性症は50歳以上の約0・9％に上る。緑藻の遺伝子はこの二つの疾病に起因する失明には有効だが、糖尿病や緑内障による失明には効果がないという。

富田准教授は「現在は人工網膜を使う治療法があるが、解像度が低いという問題がある。遺伝子治療が実現すれば、より簡単に解像度の高い視覚を回復できる可能性が高い」と話している。

研究成果は4日（日本時間5日）、米オンライン学術誌に掲載された。

Wシリーズ ヤンキース優

れ、ヤンキース（ア・リーグ優勝）が連覇を狙ったフィリーズ（ナ・リーグ優勝）を7―3で下し、4勝2敗で9年ぶり27度目のワールドチャンピオンに輝いた。ヤンキースの松井秀喜外野手（35）はこの試合で6打点を挙げる大活躍、日本選手として初めて同シリーズ最優秀選手（MVP）に選ばれた。

（4・13・25面に関連記事）

悲願の世界一を2003年の入団以来7年目で達成し、MVPで花を添えた松井秀は「最高ですね。初めてここまで来られて最高。今までで もっとも大きな思い出になる」と、MVPのトロフィーを高々と掲げ、喜びを語った。

松井秀は今シリーズ通算6え2点本塁打、三回には2点適時打、五回には右中間へ2点二塁打を放った。1試合6打点は、1960年の第3戦でのヤンキースのリチャードソンに並ぶ同シリーズ最多タイ記録。

今季が4年契約の最終年で、今後の去就が注目される松井秀。来季もヤンキースで連覇に挑むかと聞かれ、「そうなればいいと思う。僕はニューヨークが好きだし、ヤンキース、チームメートも好きだし、ファンが大好き」と話した。

米大リーグのワールドシリーズで日本選手初のMVPに選ばれ、トロフィーを掲げるヤンキースの松井秀＝5日未明、ヤンキースタジアム

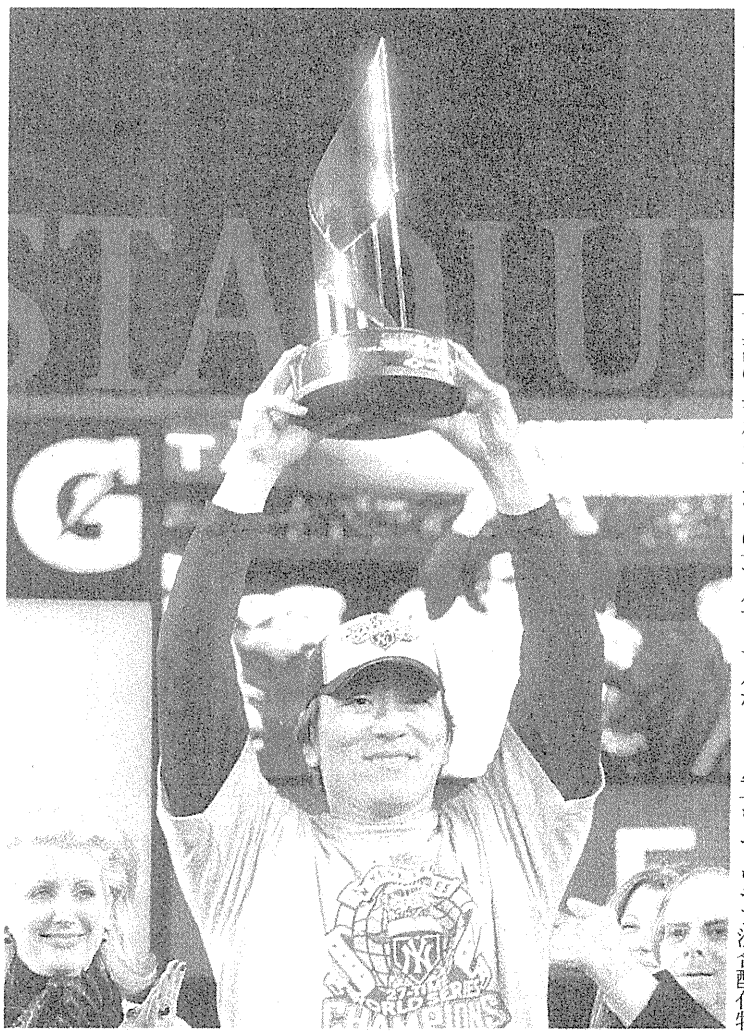

上高は上方修正したとは

プルサーマルが、5日午

ウム・ウラン混合酸化物イクル使用する国策「核燃料サイクル」は、実現に向け新たな段階に入った。

九電は午前11時に原子炉を起動。作業員が出力を調整する制御棒を徐々に引き抜き、約12時間後、臨界状態に達した。九電によると、作業は順調に進んだという。

米国務省
普天

【ワシントン共同】ケリー米国務省報道官は4日の記者会見で、米軍普

ISSN 0286-0651　2010年2月7日発行　毎月7日発行　第30巻第2号　昭和56年8月10日　第3種郵便物認可

Newton

GRAPHIC SCIENCE MAGAZINE ニュートン

素粒子を生み，宇宙を生んだ

「無」の物理学

「空っぽの空間」は，本当に空っぽなのだろうか…

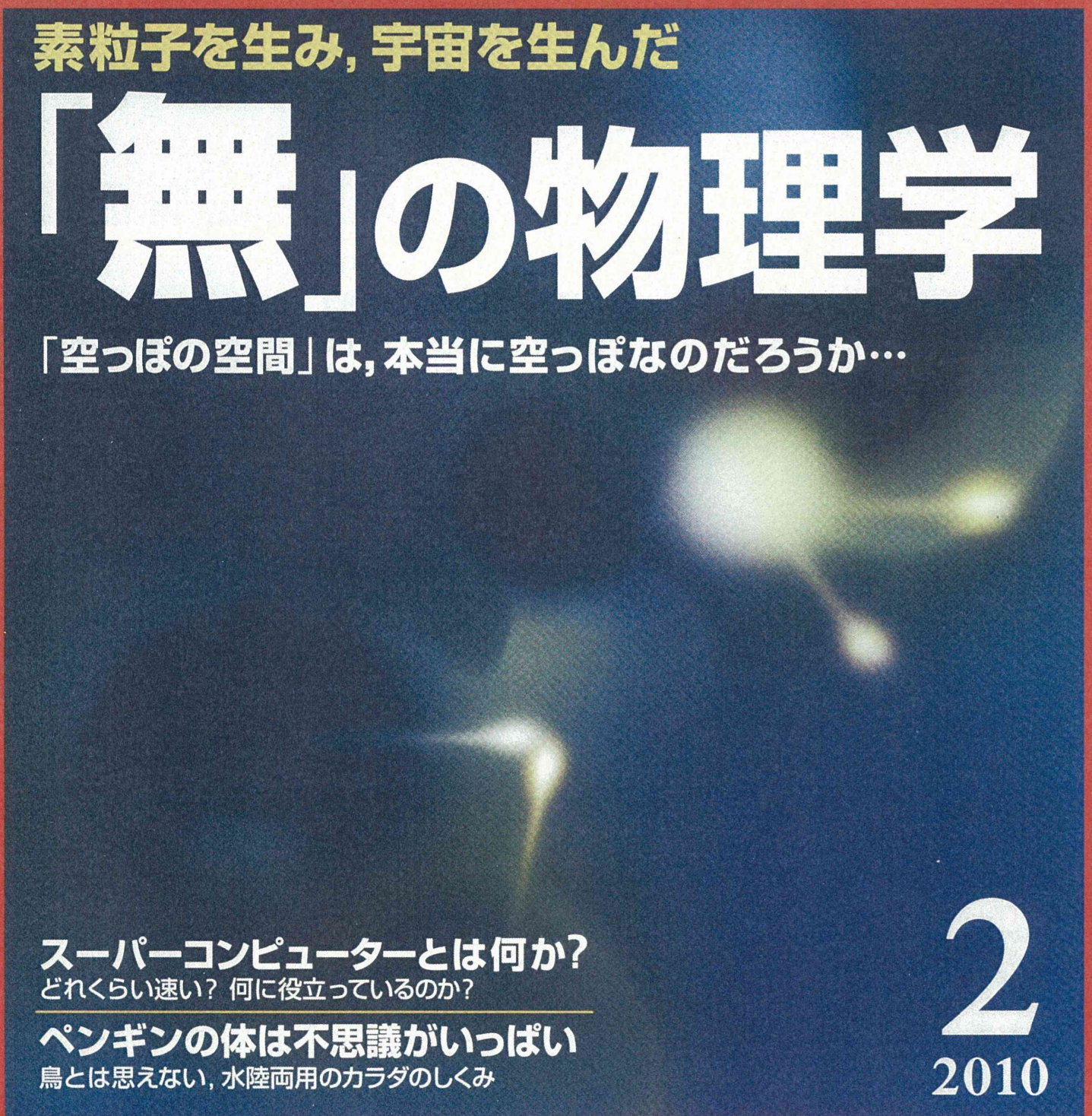

スーパーコンピューターとは何か?

どれくらい速い? 何に役立っているのか?

ペンギンの体は不思議がいっぱい

鳥とは思えない，水陸両用のカラダのしくみ

2
2010

1000円